ALMA MATER STUDIORUM
UNIVERSITÀ DI BOLOGNA

DOTTORATO DI RICERCA IN

SCIENZE E TECNOLOGIE DELLA SALUTE

Ciclo 36

Settore Concorsuale: 06/F4 - MALATTIE APPARATO LOCOMOTORE E MEDICINA FISICA E RIABILITATIVA

Settore Scientifico Disciplinare: MED/33 - MALATTIE APPARATO LOCOMOTORE

A RELIABLE AND REPRESENTATIVE SIMULATION STUDY TO INVESTIGATE THE RISK OF IMPINGEMENT IN TOTAL HIP REPLACEMENT (THR) PATIENTS.

Presentata da: Giuseppe Geraci

Coordinatore Dottorato
Igor Diemberger

Supervisore
Cesare Faldini

Co-supervisore
Marco Viceconti

Esame finale anno 2024

A RELIABLE AND REPRESENTATIVE SIMULATION STUDY TO INVESTIGATE THE RISK OF IMPINGEMENT IN TOTAL HIP REPLACEMENT (THR) PATIENTS.

ABSTRACT

Objectives

The objective of this doctoral thesis is to construct a reliable and representative, three-dimensional experimental model for the systematic evaluation of the range of motion in Total Hip Replacement (THR), through the integration of specific maneuvers at high-risk of dislocation, and contingent upon variable parameters of pelvic version. A secondary aim is to explicate the underlying mechanisms contributing to impingement phenomena by categorizing them into bone-on-bone impingement, implant-on-implant impingement, and implant-on-bone impingement.

Materials and methods

We designed a tridimensional model in a free and open-source simulation environment. The simulation routine employed an array of specialized software and methodologies to ensure both the reliability and the reproducibility of our results. Each step was meticulously conducted to ensure that the findings would not only hold scientific credibility but also offer clinically relevant insights. Different scenarios were simulated, and the range of motion of the prosthetic hip was assessed. Movements at particular risk of dislocation were assessed, and a study was conducted considering the range of motion of the femur allowed until contact (impingement) between geometries (discriminating bone-to-bone contact, implant-on-implant contact, and implant-on-bone contact). Furthermore, different pelvic version angles were evaluated to assess potential differences.

Results

The anteverted pelvis registered impingement in a greater number of movements (6 out of 9) and presented an overall reduced range of motion until geometries contact, in particular related to posterior dislocation prone movement. Conversely, the pelvic orientation with the average higher range of motion in different simulation scenarios was the neutral pelvis. The type of impingement that first occurred for most dislocation movements was the implant-on-bone contact. In contrast, the impingement that occurred at higher angles was the implant-on-implant type, which had a relevance only in pure hip extension movements.

Conclusions

The current thesis offers a methodologically rigorous and replicable experimental framework marked by both robustness and high fidelity to average anatomical and biomechanical realities.

The reported findings not only substantiate the importance of pelvic version in THR, defining higher risk for the anteverted pelvis, but also, they highlight the prominent role of implant-on-bone impingement in instability and dislocation.

Recommendations inferred from these findings have the potential to either modify or confirm current medical practice.

INTRODUCTION

Total Hip Replacement (THR) is considered the operation of the century[1]. Registry studies show over 90% success rate over a 20 years follow-up period with excellent results in relieving pain, improving function. THR is also a cost-effective procedure with a substantial reduction of the economic burden imposed by hip OA.
Despite the reported success, THR is associated with a non-negligible failure rate, and a subsequent need for revision surgery. Over the next decades the number of THR will increase, and an increasing number of revision surgeries is expected[2].
Complications are much more frequent in particular subgroups of patients, such as patients with a history of lumbar spine diseases who can develop pathological pelvic version and kinematic[3]. Also the aging of the population and the reduction of invasiveness of surgical procedures, lead more and more patients to be subjected to both THR and Lumbar Spine (LS) surgeries during lifetime, making the problem particularly prominent[4].
Lumbar spine pathology and surgery have been proposed to play a significant role on short- and long-term results of THR, being responsible for specific complications such as instability and dislocation. Patients with lumbar fusion and total hip replacement present the double of the incidence of dislocation when compared to patients only subjected to THR surgery with up to 20% incidence during lifetime[3].
Positioning of the acetabular cup represents a critical issue in patients with pathological pelvic version and kinematic because of the reduced or absent protective effect of pelvic movement. Indeed, pelvic movements allow for an effective reciprocal coupling of the acetabular cup and femoral head, even when the prosthetic components are not perfectly positioned.
Actually, the “Safe zone” for implant positioning are defined considering the position of acetabular cup and femoral stem in a static supine position, not accounting for pelvic version (the sagittal position of the pelvis: it can be anteverted or retroverted in relation to an anterior or posterior tilt) and kinematic (moving from standing to sitting position with the retroversion of the pelvis)[5].

The objective of the present doctoral thesis is to develop a robust, representative, three-dimensional experimental model aimed at investigating the THR range of motion in relation to varying parameters of pelvic version. An additional aim is to delineate the mechanisms of impingement, differentiating between osseous impingement, prosthetic impingement, and osseous-prosthetic impingement, through the incorporation of specific movements into the experimental model that are associated with a higher risk of dislocation.

ANATOMY OF THE HIP

Osseous anatomy

The pelvis, also known as the bony pelvic girdle, is an osteoarticular structure comprising the right and left coxal bones (also referred to as hip or iliac bones), the sacrum, the coccyx, and their respective articulations. This structure serves as the anatomical interface connecting the trunk to the lower limb through the coxofemoral joint.

The hip bone (also known as the innominate bone) is a flat, quadrilateral-shaped bone that is voluminous and irregular, wider at both the superior and inferior ends and narrowing at its central portion. The two contralateral bones articulate anteriorly at the pubic symphysis and posteriorly through the interposition of the sacrum at the sacroiliac joint, thereby forming the pelvic girdle. Each innominate bone consists of three distinct bones: the ilium, ischium, and pubis. In the young, these bones are connected by cartilage at the acetabular wall, a depression on the external surface that articulates with the femoral head; in adults, they are fused. Anteroinferior to the acetabulum is the obturator foramen, bounded by the ischiopubic rami.

The upper part of the hip bone is formed by the ilium, which narrows at its lower portion (ilium body) and contributes to the superior part of the acetabular cavity. It expands superiorly to form the iliac wing. Three surfaces can be distinguished: the gluteal (external), sacropelvic, and the iliac fossa (internal). The iliac fossa is separated from the sacropelvic surface by the arcuate line. The iliac tuberosity is a roughened surface situated below the posterior part of the iliac crest and is connected to the sacrum by the interosseous sacroiliac ligament. Antero-inferiorly, the auricular surface articulates with the lateral face of the sacrum.

The ischium forms the posteroinferior part of the hip bone and is divided into two portions: the body and the ramus. The body contributes to the inferior posterior part of the acetabulum and gives rise to the ramus, which proceeds anteromedially to fuse with the descending ramus of the pubis, thereby delineating the obturator foramen. The ischial tuberosity is a voluminous, roughened area on the posteroinferior aspect of the ischium, directed downward and medially. Below it lies the lesser sciatic notch.

The pubis forms the anterior part of the hip bone and articulates with its contralateral counterpart through the cartilaginous pubic symphysis. It consists of a body, a superior ramus extending posteroinferiorly to the acetabulum, and an inferior ramus, which extends inferiorly, posteriorly, and laterally to fuse with the ischial ramus. The body of the pubis has three surfaces: anterior, posterior, and symphyseal (or medial), which articulates with the contralateral pubic bone via the cartilaginous pubic symphysis.

The acetabulum is the cavity designed to accommodate the head of the femur. It is spheroidal and hollow, located at the center of the external surface of the hip bone. The inner surface of the cavity is divided into two portions: one smooth and articular, the other roughened. The non-articular portion (acetabular fossa) is quadrangular and houses the round ligament.

The obturator foramen is located antero-inferiorly to the acetabulum and is bounded by the ischium and the pubis. The shape varies between sexes, being wide and oval in males and smaller and almost triangular in females. It is almost completely obliterated by the obturator membrane, which is discontinuous in its upper part, allowing the passage of obturator vessels and nerves.

The femur is the longest and strongest bone in the human body. Its shaft is nearly cylindrical and is curved with an anterior convexity. It is narrow at the center and widens both proximally and distally. In its mid-third, the shaft has three faces and three margins: the anterior face, lateral face, and medial face. The superior part of the femur forms an

angle with the axis passing through the two condyles of approximately 10-15 degrees (angle of anteversion); the angle between the axis of the neck and the shaft measures around 125 degrees (angle of inclination or cervico-diaphyseal angle). The femoral head represents approximately two-thirds of a sphere, covered with articular cartilage, and is oriented superiorly, medially, and anteriorly. It articulates with the articular surface of the acetabulum and has a smooth surface with a small depression (fovea capitis) from which the round ligament originates.
The hip joint connects the lower limb to the pelvic girdle and consists of a ball-and-socket articulation. The spherical, convex articular surface of the femoral head articulates with the spherical, yet concave, surface of the acetabular cavity. However, the two surfaces are not equally extensive and not exactly congruent; they only fully match when the femur is in complete extension, slightly abducted, and internally rotated. The only area of the head not covered by articular cartilage is the fovea capitis, where the round ligament attaches. The depth (and thus the containment) of the acetabular cavity is increased by a fibrocartilaginous rim present on the edge of the acetabulum (acetabular labrum), which encircles even over the acetabular notch (transverse acetabular ligament).
The fibrous capsule inserts onto the rim of the acetabulum and, at the level of the acetabular notch, onto the transverse ligament; it then completely envelops the neck of the femur on the anterior side, where it attaches at the level of the intertrochanteric line, while posteriorly it ends approximately 1 cm proximally from the intertrochanteric crest. The capsule is robust and thick, especially in the superior and anterior portions where it is most stressed. Two types of bundles are recognized: the deeper ones have a circular course (orbicular zone, or Weber's annular ligament) and form a collar around the neck of the femur; longitudinal fibers prevail in the anterior and superior portions. The articular capsule is reinforced by three ligaments: iliopsoas (Bigelow's ligament, the most resistant), pubofemoral, and ischiofemoral.
The sinovial membrane lines the intra-articular portion of the neck, then reflects onto the inner surface of the capsule, covers the acetabular labrum, sheaths the round ligament, and lines the adipose tissue contained within the acetabular fossa.
The round ligament is a flat, triangular, intra-articular bundle that attaches at the level of the fovea capitis, while the base inserts on both sides of the acetabular notch, merging with the transverse ligament. At the level of the fovea, the ligament only inserts into the anterior portion, while the rest of the fossa accommodates it when it is relaxed. Accompanying arterioles and venules run through its thickness, largely destined for the head of the femur.
The iliopsoas ligament is triangular in shape and very strong; it is located anterior to the joint and is intimately fused with the longitudinal bundles of the capsule. It runs between the anterior inferior iliac spine and the edge of the acetabulum, where it attaches at the apex, extending to the intertrochanteric line where the base of the ligament inserts; due to its shape, it is also known as Bigelow's Y ligament. The vertically running bundle becomes tense during the extension of the thigh over the pelvis, limiting its movement.
The pubofemoral ligament is also triangular, originating from the iliopectineal eminence of the superior ramus of the pubis and the obturator crest, while the apex moves downward where it fuses with the fibrous capsule and the deep part of the iliopsoas ligament, ending above the lesser trochanter. This ligament becomes tense during the abduction of the thigh, limiting its movement.
Posteriorly, the capsule is reinforced by the ischiofemoral ligament. The bundles constituting it originate from the posterior inferior edge of the acetabular rim and run in a spiral direction upward and outward on the posterior superior face of the neck. Some bundles merge with the orbicular zone of the capsule, others insert onto the greater trochanter, on a deeper plane compared to the iliopsoas ligament.

Blood supply to the joint is provided by two arteries: the deep femoral and the internal iliac. From the deep femoral arise the two circumflex arteries, which encircle the femur creating an anastomosis. From the internal iliac arise the obturator, ischiatic, and gluteal arteries. The nerves come from the femoral, obturator, and superior gluteal.

Muscles of the Iliac Region

This region consists of two muscles originating from the final section of the spine (major psoas) and the iliac bone (iliacus), both inserting onto the femur and acting as flexors of the thigh and spine. A third muscle (minor psoas), absent in 40% of individuals, originates from the last lumbar vertebrae and, attaching to the lumbosacral spine, does not act on the femur. The major psoas and iliacus muscles originate separately but unite inferiorly to attach at a common site on the lesser trochanter. They are often collectively referred to as the iliopsoas muscle.

The major psoas is a lengthy muscle situated laterally to the lumbar segment of the spinal column and the superior aperture of the pelvis. It originates from the transverse processes of all lumbar vertebrae, and from the lateral surfaces of vertebrae from T12 to L4, and their respective intervertebral discs. These origins form fibrous arches that are concave medially, bridging vertebral bodies and creating spaces for lumbar arteries, veins, and sympathetic nerve fibers. The muscle exits the pelvis through a notch on the anterior edge of the iliac bone and attaches to the lesser trochanter of the femur.

The iliacus muscle is a muscular sheet originating from the upper two-thirds of the iliac fossa, the inner lip of the iliac crest, and the upper part of the sacral wing. Muscle bundles converge medially to unite with the fibers of the major psoas, forming a shared tendon inserting on the lesser trochanter. Innervation is provided by the ventral branches of lumbar spinal nerves L1, L2, L3, and vascularization derives from branches of the lumbar arteries, common iliac artery, external iliac artery, femoral artery, and medial circumflex artery. In addition to thigh flexion, the muscle also performs external rotation.

Muscles of the Gluteal Region

This region comprises nine muscles (gluteus maximus, gluteus medius, and gluteus minimus, piriformis, internal and external obturator, superior and inferior gemellus, and quadratus femoris) that originate in the pelvic basin and insert onto the femur.

The gluteus maximus is the most superficial muscle in this region. It originates from the posterior gluteal line of the iliac wing, the bony surface posterior-superior to it, the posterior face of the sacrum, the coccyx, and the sacrotuberous ligament. Its fibers descend laterally; the more superficial fibers continue into the fascia lata, while the deeper part inserts onto the gluteal tuberosity on the femur. This muscle acts to extend and externally rotate the femur while extending the trunk by anchoring itself to the femur, playing a significant role in maintaining an upright posture. Vascularization is supplied by the superior and inferior gluteal arteries, and innervation is provided by the inferior gluteal nerve (L5 and S1).

The gluteus medius is a broad, thick muscle, covered by the gluteus maximus posteriorly and by deep fascia anteriorly. It originates from the external surface of the iliac wing, between the iliac crest, the posterior gluteal line, and the anterior gluteal line. Its fibers converge into a flat tendon that inserts onto the upper and posterior part of the greater trochanter. Blood supply is from the superior gluteal artery, and innervation is from the superior gluteal nerve (L4 and L5).

Located deep to the gluteus medius, the gluteus minimus has a fan-shaped structure and originates from the external surface of the ilium between the anterior and inferior gluteal lines. Its fibers converge into a tendon that inserts onto the anterior surface of the greater

trochanter. Like the gluteus medius, it is vascularized by the superior gluteal artery and innervated by the superior gluteal nerve (L4 and L5).
Both the gluteus medius and gluteus minimus abduct the thigh while internally rotating it when anchored to the pelvis. They play an important role in maintaining an erect trunk and horizontal pelvis when the contralateral limb is lifted from the ground.
The piriformis is located on the same plane as the gluteus medius. It originates from the lateral portion of the anterior surface of the sacrum and from the gluteal surface of the ilium, near the posterior-inferior iliac spine. The muscle fibers exit the pelvis through the greater sciatic foramen and insert onto the superior margin of the greater trochanter. Often, the tendon of this muscle, which in some cases may be fused with the gluteus medius, partially joins the common tendon of the internal obturator and the gemelli. The muscle functions in the external rotation of the thigh when the hip is extended and in its abduction when it is flexed. Innervation is supplied by branches from L5 and S1, and blood supply is from the gluteal artery.
The internal obturator originates from the inner surface of the obturator membrane, which covers the obturator foramen, and from the margins of the foramen itself. The muscle fibers converge toward the lesser sciatic foramen and terminate in ribbon-like tendons that reflect at a right angle at the level of the ischial notch. A bursa is interposed between this and the muscle fibers of the internal obturator. The fibers come together in a single flat tendon that crosses posteriorly to the articular capsule to insert, along with the superior and inferior gemelli, onto the medial surface of the greater trochanter, anterior and superior to the trochanteric fossa. The muscle functions as an external rotator of the thigh, like the gemelli. It receives branches from the obturator and ischiatic arteries; the nerve for the internal obturator originates from L5 and S1.
The superior gemellus is the smaller of the two gemellus muscles. It originates from the posterior surface of the ischial spine, adheres to the tendon of the internal obturator, and along with this and the inferior gemellus, inserts onto the medial face of the greater trochanter. At times, it may be absent or indistinguishable.
The inferior gemellus originates from the upper part of the ischial tuberosity, below the groove for the tendon of the internal obturator, and with the superior gemellus and internal obturator, inserts onto the medial face of the greater trochanter. Like the internal obturator, which the gemelli may be considered accessory muscles to, they externally rotate the thigh when extended and abduct it when flexed. Innervation is supplied from the roots of L5 and S1: the superior gemellus through the nerve to the internal obturator and the inferior gemellus through the nerve to the quadratus femoris; they receive vascularization from branches of the ischiatic and obturator arteries.
The quadratus femoris is a flat, quadrangular muscle, located between the inferior gemellus and the superior margin of the adductor magnus, from which it is separated by the transverse branch of the circumflex femoral artery. It originates from the upper part of the external surface of the ischial tuberosity and passes behind the hip joint and the femoral neck to insert onto the intertrochanteric crest, approximately in its middle section. The quadratus femoris also functions as an external rotator of the thigh. It is innervated by the nerve to the quadratus femoris (L5 and S1) and receives branches from the ischiatic artery and the first perforating artery of the deep femoral.
The external obturator is a flattened, triangular-shaped muscle; it originates from the two medial thirds of the external surface of the obturator membrane. The tendon passes behind the articular capsule to terminate in the trochanteric fossa of the femur. It functions as an external rotator of the thigh. Vascularization is supplied by the obturator artery; innervation is received from the roots of L3 and L4, via the obturator nerve.

Muscles of the Anterior Thigh Region

This group consists of the tensor fasciae latae, sartorius, and rectus femoris, which act on both the hip and knee joints, as well as the vastus medialis, vastus lateralis, and vastus intermedius, which act only on the knee joint.
The tensor fasciae latae is situated in the upper external part of the thigh; it is a thin and flat muscle. It originates from the anterior edge of the lateral lip of the iliac crest, from the lateral surface of the anterior superior iliac spine, and from the underlying notch. It inserts between the middle and upper thirds of the thigh onto the iliotibial tract. It is vascularized by the superior and inferior gluteal arteries and is innervated by the superior gluteal nerve (L4 and L5). Via the iliotibial tract, it extends the leg and externally rotates it; it also participates in the abduction and internal rotation of the thigh. In a standing posture, it contributes to pelvic stabilization.

The sartorius is a narrow, ribbon-like muscle. It originates from the anterior superior iliac spine and the upper half of the underlying notch; it crosses the thigh obliquely and descends vertically to the medial side of the knee. The muscle fibers continue into a flat tendon that expands into a broad aponeurosis attached to the upper part of the medial margin of the tibia, anterior to the gracilis and semitendinosus muscles (forming the pes anserinus). The muscle contributes to the flexion of the leg on the thigh and the thigh on the pelvis. It also participates in the abduction and external rotation of the thigh. It is innervated by the femoral nerve (L2 and L3), particularly its muscular cutaneous external branch; it receives arterial branches from the femoral artery.
The quadriceps femoris almost completely covers the femur anteriorly, medially, and laterally; its four main components can be distinguished: rectus femoris, vastus lateralis, vastus medialis, and vastus intermedius. The rectus femoris is the only biarticular muscle, crossing both the hip and knee joints, while the other three cross only the knee joint. The tendons of the four muscles join in the lower part of the thigh to form the quadriceps tendon, which incorporates and attaches to the patella. From this, the patellar (or patellar) ligament extends to the anterior tibial tuberosity.
The rectus femoris originates with two tendons: one direct from the anterior inferior iliac spine, and one reflected, flat, and thinner, originating from a fossa above the acetabulum and from the fibrous capsule of the hip joint. The muscle ends with a broad, thick aponeurosis that gradually narrows into a flattened tendon, which inserts onto the base of the patella as the central and superficial part of the quadriceps tendon.
The vastus lateralis is the most voluminous component of the quadriceps femoris; it originates with a broad aponeurosis from the intertrochanteric line. The muscle mass continues distally with a robust aponeurosis that narrows into a flat tendon and inserts onto the base and lateral margin of the patella.
The vastus medialis originates from the lower part of the intertrochanteric line, from the spiral line, and from the medial lip of the linea aspera; most fibers insert onto the medial margin of the patella.
The vastus intermedius originates from the lateral and anterior surfaces of the proximal two-thirds of the femoral shaft; its bundles terminate in an aponeurosis that attaches to the lateral margin of the patella and to the lateral condyle of the tibia. The articular muscle of the knee may either be separate or fused with the vastus intermedius; it consists of bundles that originate from the anterior surface of the distal femur and insert into a superior recess of the synovial joint membrane of the knee.
The quadriceps femoris and the articular muscle of the knee are innervated by the femoral nerve (L3 and L4); they receive branches from the deep femoral artery, from the perforating arteries, and from the knee joint arteries. The action of the quadriceps consists of extending the leg on the thigh; additionally, the rectus femoris contributes to flexing the thigh on the pelvis or, if the thigh is maintained as a fixed point, to flex the pelvis.

THIGH MUSCLES: MEDIAL GROUP

All the muscles belonging to the medial group of the thigh (gracilis, pectineus, long adductor, short adductor, and large adductor) straddle the hip joint, but only the gracilis crosses the knee joint as well.

The gracilis is the most superficial muscle in this group, being thin and flat. It originates from a slender aponeurosis from the medial margin of the lower half of the pubic body and the adjacent ascending ramus of the ischium. The fibers descend vertically, converging into a cylindrical tendon that crosses the medial femoral condyle and medial tibial plateau, where it fans out and inserts into the upper part of the medial surface of the tibia. It is innervated by fibers from the obturator nerve (L2) and is vascularized by the obturator artery. The gracilis flexes the leg and rotates it internally; it also contributes to the adduction of the thigh.

The pectineus is a flat, quadrangular muscle found in the femoral triangle. It originates from the pectineal crest of the pubis; its fibers run downward, backward, and laterally to insert along the line connecting the lesser trochanter to the linea aspra (pectineal line). It is innervated by the femoral nerve (L2 and L3); vascularization comes from the obturator artery and the femoral circumflex artery. The pectineus adducts the thigh and flexes it on the pelvis.

The long adductor is the most anterior among the three adductor muscles; it is a broad, fan-shaped muscle. It originates with a narrow, flat tendon from the body of the pubis, at the angle between the pubic crest and the pubic symphysis. It expands into a broad muscular belly that runs downward, backward, and laterally to insert with an aponeurosis on the linea aspra, at the level of the middle third of the diaphysis. Blood supply is provided by the femoral artery; it is innervated by fibers from the anterior branch of the obturator nerve (L2, L3).

The short adductor originates from the external surface of the pubic body; it has a triangular shape and runs backward, laterally, and downward to insert onto the femur along a line extending from the lesser trochanter to the linea aspra. It is vascularized by the femoral artery and is innervated by the obturator nerve (L2 and L3).

The large adductor is a robust, triangular muscle that originates from the lower ramus of the pubis, the lower ramus of the ischium, and the inferior lateral aspect of the ischial tuberosity. The part originating at the pubic ramus runs almost horizontally to insert on the femur's gluteal tuberosity and lies on an anterior plane. The fibers originating from the ischium's lower ramus fan out downward and laterally to attach with a long aponeurosis to the linea aspra and the proximal part of the medial supracondylar line. The middle portion of the muscle, primarily consisting of fibers originating from the ischial tuberosity, descends almost vertically and terminates around the lower third of the thigh, where it continues into a cylindrical tendon that inserts into the medial condyle. The long insertion of the muscle is interrupted by a series of orifices, delimited by fibrous arches that attach to the bone. It is vascularized by the femoral artery and is innervated by the obturator nerve and the tibial component of the sciatic nerve (L2, L3, L4).

The primary action of these muscles is the adduction of the thigh, mainly acting as synergists in the complex mechanisms of locomotion and partially controlling posture. Additionally, the large adductor and the long adductor are internal rotators of the thigh.

THIGH MUSCLES: POSTERIOR GROUP

The posterior muscle group of the thigh comprises the biceps femoris, semitendinosus, and semimembranosus muscles. These muscles span across both the hip and knee joints and are responsible for extension at the coxofemoral joint and flexion at the knee joint.
The biceps femoris is situated in the posterolateral region of the thigh. It has dual origins: the long head originates from the upper portion of the ischial tuberosity, sharing a common tendon with the semitendinosus. The short head, which may be absent, arises from the lateral lip of the linea aspra and the lateral supracondylar line. The muscle fibers of the long head form a fusiform muscle belly that descends laterally, crossing the sciatic nerve. These fibers continue into an aponeurosis onto which the fibers of the short head also attach. The muscle then narrows and continues into a tendon that bifurcates; the larger part wraps around the lateral collateral ligament and attaches to the fibular head, while the remaining fibers insert into the lateral condyle of the tibia. It is innervated by the sciatic nerve (L5, S1) and receives vascular supply from branches of the ischiatic artery, internal pudendal artery, circumflex femoral artery, and perforating arteries.
The semitendinosus is located in the posteromedial region of the thigh, the semitendinosus originates from the upper portion of the ischial tuberosity, sharing a common tendon with the long head of the biceps femoris. The muscle belly is fusiform and ends slightly below the midpoint of the thigh with a long tendon that courses along the surface of the semimembranosus. This tendon then wraps around the medial condyle of the tibia, passing over the medial collateral ligament (from which it is separated by a bursa) and inserts into the upper part of the medial surface of the tibia, posterior to the sartorius insertion and distal to the gracilis insertion. It is innervated by the sciatic nerve (L5, S1) and is vascularized by branches of the ischiatic artery, internal pudendal artery, circumflex femoral artery, and perforating arteries.
The semimembranosus is positioned in the posteromedial region of the thigh. It originates from a long, flat tendon from the ischial tuberosity, laterally adjacent to the tendons of the biceps femoris and semitendinosus. This tendon runs medially adjacent to the adductor magnus and expands into an aponeurosis that extends inferiorly, deep to the semitendinosus. At about the midpoint of the thigh, muscle fibers emanate from the tendon and converge into another aponeurosis, which narrows and transforms into a tendon that inserts onto the tubercle located on the posterior surface of the medial tibial condyle. It is innervated by the sciatic nerve (L5, S1) and vascularized by branches of the ischiatic artery, internal pudendal artery, circumflex femoral artery, and perforating arteries.
Functionally, when taking the femur as a fixed point, the posterior thigh muscles flex the leg at the knee. When taking the pelvis as a fixed point, they serve as extensors at the coxofemoral joint, acting as antigravity muscles. With the knee in a semi-flexed position, the biceps femoris serves as an external rotator, while the semimembranosus and semitendinosus act as internal rotators.

Arteries of the Thigh

The arteries that supply the musculoskeletal components of the hip joint are derived from the internal iliac arteries (obturator artery, and superior and inferior gluteal arteries) and the external iliac artery (femoral artery).
The obturator artery originates from the anterior trunk of the internal iliac artery, proceeding anteriorly and inferiorly against the lateral wall of the pelvis, from which it exits through the obturator foramen. Prior to exiting the pelvis, it provides iliac branches that vascularize the iliac bone and muscle, and a pubic branch that anastomoses with the contralateral branch. Outside the pelvis, the artery bifurcates into an anterior and a posterior branch. The former supplies branches to the external obturator, pectineus, adductor, and gracilis muscles, and anastomoses with the posterior branch and the medial circumflex artery of the femur. The posterior branch vascularizes the posterior muscles,

which attach to the ischial tuberosity, and anastomoses with the inferior gluteal artery. It also provides an acetabular branch, which enters the joint through the acetabular notch.
The inferior gluteal artery represents the largest division branch of the internal iliac artery; it vascularizes the buttock region and the posterior thigh. Descending in front of the sacral plexus and the piriformis, it exits the pelvis through the greater sciatic foramen. It descends between the greater trochanter and the ischial tuberosity, continuing inferiorly in the posterior part of the thigh, vascularizing the skin and anastomosing with branches of the perforating arteries. Within the pelvis, it provides branches for the piriformis muscle, and externally vascularizes the greater gluteus, the internal obturator, the gemellus, the quadratus femoris, and the upper portion of the thigh muscles. Frequently, there is a joint branch for the hip joint.
From the posterior trunk of the internal iliac artery mainly two arteries arise: the ileolumbar artery and the superior gluteal artery. The former is directed to the iliopsoas muscle; the latter, within the pelvis, vascularizes the piriformis and the internal obturator.
The femoral artery is the continuation of the external iliac artery; it takes this name after crossing the inguinal ligament and runs inferiorly on the anteromedial aspect of the thigh, in the femoral triangle. The limits of this triangle are laterally defined by the medial edge of the sartorius, medially by the medial edge of the long adductor, and superiorly by the inguinal ligament. The floor of the triangle is laterally formed by the iliopsoas and medially by the pectineus. The femoral vein is located medially to the artery, the nerve laterally. At the boundary between the middle and lower thirds of the thigh, the artery passes through the adductor canal to become the popliteal artery. This canal is an aponeurotic tunnel extending from the apex of the femoral triangle to the orifice of the great adductor, through which the femoral vessels pass into the popliteal fossa. In its proximal tract, it gives off several branches: the superficial epigastric artery, the superficial circumflex iliac artery, the superficial external pudendal artery, and deep branches and some muscular branches for the sartorius, the vastus medialis, and the adductor muscles.
The deep femoral artery is a large branch that originates from the lateral wall of the femoral artery approximately 3-5 cm from its origin. It proceeds medially to the femur, where it courses between the pectineus and long adductor muscles and then between the latter and the short adductor; it continues to descend between the long and great adductors where it terminates by perforating the latter to proceed into the popliteal fossa. In its upper tract, it forms an important anastomosis between the internal and external iliac arteries. The lateral circumflex femoral artery vascularizes the greater trochanter and forms, along with branches of the medial circumflex femoral artery, an anastomotic ring that encircles the base of the femoral neck, supplying branches to the head and neck, penetrating the articular capsule in its posterolateral portion. The medial circumflex femoral artery can also originate from the femoral artery; it participates in the anastomotic circulation around the neck of the femur.
The perforating arteries are usually three in number and perforate the insertion of the great adductor to reach the posterior region of the thigh. The first perforating artery moves backward between the pectineus and short adductor to distribute to the short adductor, the great adductor, and anastomoses with the inferior gluteal, medial and lateral circumflex femoral arteries, and the second perforating artery. The second perforating artery passes through the insertions of the short and great adductors and divides into branches for the vascularization of the muscles of the posterior thigh region, also giving off the nutrient artery of the femur. The third perforating artery passes through the insertion of the great adductor and divides into branches directed to the posterior thigh muscles. The last tract of the deep femoral artery is known as the fourth perforating artery.

Nerves of the Thigh

The lumbar plexus is situated posterior to the major psoas muscle and anterior to the transverse processes of the lumbar vertebrae. It is composed of the anterior roots of L1, L2, L3, portions of the roots of T12, and most of L4. The plexus is organized into a series of loops: the first lumbar branch anastomoses with both the twelfth thoracic and the anterior branch of the second lumbar (origin of the iliohypogastric and ilioinguinal nerves); the second anastomoses with the third, giving rise to the lateral femoral cutaneous and genitofemoral nerves; the third anastomoses with the fourth and continues into the femoral nerve; the fourth is divided into three branches: an ascending one contributing to the formation of the femoral nerve, a medial one constituting the primary portion of the obturator nerve, and a descending one contributing to the formation of the sacral plexus. The initial branches that arise are the iliohypogastric and ilioinguinal (L1) and the genitofemoral (L1 and L2).
The obturator nerve originates from the anterior division of the anterior branches of L2, L3, and L4; it descends within the thickness of the major psoas muscle and exits from its medial margin at the level of the superior aperture of the pelvis. It proceeds anteriorly and inferiorly along the lateral wall of the lesser pelvis, adherent to the internal obturator muscle, until it reaches the obturator foramen through which it enters the thigh. At this level, it divides into an anterior and a posterior branch; the anterior branch passes anterior to the external obturator and descends in the thigh in front of the short adductor and behind the pectineus and long adductor muscles. It supplies the long adductor, gracilis, short adductor, and pectineus muscles. The posterior branch traverses the anterior wall of the external obturator, which it innervates, and passes behind the short adductor and in front of the great adductor, to which it is distributed.
The femoral nerve is a sensory and motor nerve originating from the posterior division of the anterior branches of L2, L3, L4. It descends through the muscle bundles of the major psoas, from whose inferior lateral margin it emerges; it continues downward between the psoas and iliac muscles, passing behind the inguinal ligament to enter the thigh. At this level, it divides into four branches: the lateral and medial muscular cutaneous nerves positioned anteriorly, the saphenous nerve, and the quadriceps nerve positioned posteriorly.
The lateral muscular cutaneous nerve moves downward and laterally, between the psoas and sartorius muscles, giving rise to muscular branches for the sartorius muscle and cutaneous branches for the anteromedial surface of the knee.
The medial muscular cutaneous nerve divides into cutaneous branches for the superomedial region of the thigh and muscular branches for the pectineus muscle. The quadriceps nerve is a deep branch that further divides into four branches, each serving one of the four parts of the muscle.
The saphenous nerve is an exclusively sensory nerve that runs in the adductor canal, then becomes superficial on the external surface of the lower part of the thigh and knee, where it divides into its two terminal branches: the infrapatellar and tibial nerves.
The sacral plexus is formed by the anterior branches of the first, second, and third sacral nerves, part of the anterior branch of the fourth, and the lumbosacral trunk. The anterior branches of these nerves converge at the level of the large ischial foramen and join, without significant exchange of fascicles, into an upper portion, given by the lumbosacral trunk and the first, second, and part of the third sacral nerve, continuing into the sciatic nerve, and a lower, thinner portion, given by the remaining part of the third and part of the fourth, which continues into the pudendal nerve. Before forming the sciatic nerve, several nerves originate that are responsible for the innervation of specific muscles of the region: the nerve for the quadratus femoris and inferior gemellus, the nerve for the internal obturator and superior gemellus, that for the piriformis, the superior and inferior gluteal nerves, and a sensory nerve, the posterior cutaneous nerve.

The sciatic or ischiatic nerve is the largest nerve in the human body and represents the continuation of the sacral plexus. It exits the pelvis through the large ischial foramen and descends between the great trochanter and the ischial tuberosity, in the posterior region of the thigh down to the lower third, where it divides into two terminal branches: the tibial nerve (or internal popliteal sciatic) and the common peroneal nerve (external popliteal sciatic). In its upper portion, it is situated deeply relative to the great gluteus and the piriformis; it then passes over the quadratus femoris, which separates it from the hip joint. More distally, it is situated behind the great adductor. The muscular branches of the nerve are directed to the biceps femoris.

TOTAL HIP REPLACEMENT

The prosthetic replacement of the hip joint is heralded as the surgical intervention of the century, owing to its high success rates and significant improvement in the patients' quality of life who undergo this treatment. Hip replacement remains the treatment of choice for patients with severe joint destruction accompanied by limitations in movement and functional disability.
Three principal types of hip prostheses exist:

- Hemiarthroplasties or partial prostheses, which only replace the proximal epiphysis of the femur. They consist of a femoral stem and a hemispherical head articulating directly within the acetabulum (unipolar hemiarthroplasty) or a head articulating within a cup lodged in the acetabular cavity (bipolar hemiarthroplasties).
- Total hip arthroplasties, which replace both articular surfaces—namely the proximal epiphysis of the femur and the acetabulum.
- Resurfacing prostheses, which also replace both articular surfaces but conserve the proximal femoral bone, merely "resurfacing" it.

Hemiarthroplasties, also known as partial prostheses, replace only the proximal epiphysis of the femur. Structured as a stem inserted into the femur and a hemispherical head replacing the bony head of the femur, the surface may articulate either with the native acetabulum or within a cup lodged in the acetabulum. The primary drawback of this type lies in the joint's limited stability, making it unsuitable for younger patients with high functional demands. It is not recommended for patients with primary hip osteoarthritis, as advanced-stage patients often already have compromised acetabula. However, it remains the preferred choice for elderly patients with femoral neck fractures, offering shorter surgical time and quicker postoperative recovery.
Total hip arthroplasties aim to replace both articulating surfaces of the hip. The prosthesis consists of an acetabular cup, liner, femoral head, and stem. The acetabular component is usually hemispherical or elliptical and is affixed using screws, cement, or a press-fit technique. Between the cup and the head lies the liner, a prosthetic structure made from various materials like ceramic, metal, or polyethylene, enhancing the prosthesis's overall stability.
Resurfacing prostheses preserve the proximal epiphysis of the femur and involve metal surfaces covering both the femoral and acetabular articulating surfaces. They offer advantages in load distribution, thus reducing the risk of dislocation. However, from a surgical standpoint, a larger incision is required for implantation, and there is an increased risk of femoral neck fractures.
All prostheses are constructed from metallic alloys designed to withstand loading forces. They adhere to the bone to achieve implant fixation, which can be either biological or cemented.
Biological fixation necessitates that the bone cavity for the prosthesis closely mirrors the implant's shape and is slightly smaller to promote primary stability (press-fit). The material must not only be biocompatible but also osteoconductive, facilitating osteointegration and subsequent secondary stability achieved within approximately six weeks.
Cemented fixation requires the bone cavity to correspond to the implant's shape but be slightly larger to accommodate a layer of cement. The cement is a polymethylmethacrylate (PMMA) acrylic resin that, when mixed with a catalyst, initially assumes a viscous

consistency. It subsequently hardens due to an exothermic reaction, permanently fixing the prosthesis to the bone.
Articular movement in total and resurfacing hip arthroplasties is facilitated by the head sliding within the acetabular insert or liner. Prosthetic coupling can be "hard-on-soft," where a hard head made of metal or ceramic articulates with a soft liner made of polyethylene, or "hard-on-hard," where both the head and liner are made of hard materials. Hard-on-hard couplings (Metal-on-Metal, Ceramic-on-Ceramic) have high resistance to wear but are prone to brittleness, while hard-on-soft couplings are less likely to break but may undergo more wear over time.

HISTORY OF PROSTHETIC REPLACEMENT AND CURRENT DEVELOPMENTS

The modern conception of hip prosthesis was introduced by Sir John Charnley in the 1960s. He pioneered the use of the metal-polyethylene pairing with small-sized heads and the cementation of prosthetic components using an acrylic cement, polymethylmethacrylate (PMMA). These innovations overcame the limitations of previous technologies, increasing implant longevity and substantially improving clinical outcomes. The prosthetic fixation to the bone was achieved.
Charnley's prosthesis was also characterized by the use of a monoblock femoral stem made of a metallic alloy, resulting in a low-friction metal-polyethylene prosthesis, conceptually identical to those used today.
From the 1960s to the present, numerous innovations have rendered the technologies introduced by Charnley obsolete. The development of ultra-high molecular weight polyethylenes, cross-linked and added with Vitamin E, as well as the introduction of new surfaces like ceramic, have virtually resolved the wear issue. Moreover, the study of osteointegration capabilities and biocompatibility of various materials, in the form of coatings or surface treatments, has reserved cementation for specific cases where the patient's biological potential is irreparably compromised. Recently, the assistance of 3D printers has allowed for the additive technology reproduction of the characteristic porosity of cancellous bone.
In recent years, innovations have been directed not only at prosthetic design but also in the search for minimally invasive surgical approaches to minimize soft tissue damage, reduce perioperative complications, and expedite functional recovery of the operated lower limb.

Indications for Hip Replacement and Clinical-Diagnostic Evaluations

Hip replacement serves as the treatment of choice for various pathological conditions of the hip joint, including primary hip osteoarthritis, avascular osteonecrosis of the femoral head, congenital hip dysplasia, slipped capital femoral epiphysis, rheumatoid arthritis, and other seronegative autoimmune arthritides. These conditions are characterized by arthritic degeneration of the joint. Another significant indication for hip replacement is medial femoral neck fractures. The primary aim of the surgical procedure is to alleviate pain, enhance joint mobility, and improve overall function, thereby elevating the patient's quality of life.
Absolute contraindications encompass local or systemic infectious states or severe comorbidities such as multi-organ failure, severe cardiovascular, respiratory, renal, and metabolic diseases. Neuromuscular disorders often constitute a relative contraindication for hip replacement due to the elevated risk of postoperative complications like prosthetic dislocation.

Clinical Evaluation

Once the decision for hip replacement is made, a comprehensive preoperative assessment of the patient is imperative. A detailed remote pathological history should seek to identify any absolute contraindications to the surgery, such as severe multi-organ insufficiencies that heighten perioperative mortality risk. The presence of significant cardiovascular, respiratory, renal, and metabolic conditions may necessitate a pre-admission anesthesiological evaluation and specialized consultations. Furthermore, it is critical to examine any history of generalized or localized infections (e.g., urological, dental) that are either episodic or recurrent. Moreover, it is vital to investigate previous orthopedic conditions like fractures or joint deformities that might complicate the surgical procedure.

Physiological anamnesis should assess the patient's body habitus, potential presence of obesity, and muscular status. Information about the patient's profession, involvement in sports, and lifestyle habits will aid in understanding functional demands and surgical expectations. It is useful to inquire about ongoing pharmacological treatments (particularly anticoagulants or immunosuppressants requiring cessation or substitution before surgery) and lifestyle habits like smoking and alcohol consumption, as hospitalization could exacerbate withdrawal symptoms.

Recent pathological anamnesis should focus on the clinical condition of the hip to be operated upon: the onset of pain, duration of limping, and previous unsuccessful conservative treatments. Surgical indications are typically reserved for patients with chronic pain persisting for at least six months and unresponsive to pharmacological conservative therapy. Additionally, it is essential to ascertain that the patient has not undergone intra-articular hip injections within the preceding three months to minimize the risk of local infection.

The general physical examination should evaluate the patient's posture while standing and walking. The type of limp (escape or ankylosis), any anatomical, functional, or perceived leg-length discrepancies should be determined. The potential for correcting such discrepancies should be communicated to the patient, noting that corrections exceeding 2 cm in lengthening substantially increase the risk of neurovascular stretching complications, and shortening beyond 1 cm significantly elevates the risk of dislocation.

Lastly, the assessment should include spinal alignment, especially on the sagittal plane, and pelvic anteversion. Concerning muscle tone and trophism, alterations (particularly in the gluteal muscles) can severely compromise implant stability. The range of motion should be assessed in all planes and communicated to the patient, explaining that greater motion restriction implies a lengthier rehabilitation process. Severe articular stiffness, as observed in advanced osteoarthritis, can complicate intraoperative dislocation maneuvers.

Patient's functional requirements must be considered in light of their age, muscle state, body mass, profession, and sports activities. The patient should be questioned about the duration of pain and/or disability, particularly the duration of symptoms, any conservative therapy, or intra-articular injections.

RADIOLOGICAL ASSESSMENT

Instrumental evaluation is crucial for the proper diagnostic framing of the patient and for preoperative planning. During the diagnostic pathway, the patient often presents at the orthopedic consultation already in possession of a radiographic report. For the purposes of preoperative evaluation, it is essential to visualize the hip in an anteroposterior radiograph. In this manner, one can not only elucidate the etiology but also assess the surface of both joint ends, detect any acetabular dysmorphisms, and proactively plan for the ideal prosthetic implant to restore the geometric integrity of the pelvis.

Preoperative planning is executed on an anteroposterior pelvis radiograph: if the hip to be operated on is fixed in an incongruous position, planning can be conducted on the contralateral hip. Planning involves measuring the osseous surfaces of the acetabular cavity and the proximal femur to select the most suitable prosthetic implant for restoring the correct articular geometry of the hip. At the acetabular level, one must observe any dysmorphisms, deficiencies in the acetabular walls (crossover sign, center of rotation-to-posterior wall ratio), osteophytosis, and degree of acetabular protrusion. The radiographic teardrop serves as the reference marker, which in vivo is identifiable through the transverse acetabular ligament.

The acetabular component should approximate the size of the native socket as closely as possible, following adequate removal of sclerosis: this generally corresponds to one, or at most two, sizes larger than the diameter of the femoral head. Additional considerations on measurements can be made based on the implant (choice of a larger diameter head, resurfacing prostheses). The socket should be positioned at 40-45° of inclination relative to a line passing through the radiographic teardrops; it should not be uncovered by bone for more than one-third of its surface and should restore the physiological center of rotation as much as possible.

At the femoral level, the osteotomy of the neck should be planned according to the type of stem: the typical section is 1 cm proximal to the lesser trochanter and inclined at 45° relative to the longitudinal axis of the femur, although some prosthetic designs require more conservative cuts. The implant should be positioned with the junction between the neck of the prosthesis and the stem at the level of the femoral head osteotomy, selecting the most appropriate size to ensure optimal filling of the femoral canal.

If variable neck geometry implants or modular prostheses are available (with options to select designs with standard or lateralized geometry), it is necessary to monitor the cervico-diaphyseal angle of the femur to be operated on by calculating the offset. One then tests the various components, assessing the offset, the center of rotation of the acetabulum, and the limb length, with the aim of selecting the most suitable type of implant.

FIXATION TYPE: CEMENTED AND UNCEMENTED PROSTHESES

The selection of the implant is made based on the pathological anatomy of the hip, the general characteristics (age, medical history, functional requirements) of the patient, and the preferences of the surgeon. Foremost, it is essential to choose the type of fixation to employ: biological or cemented. To date, no clear superiority of one implant type over the other has been demonstrated. On one hand, cemented prostheses ensure immediate fixation of the implant, allowing the patient to ambulate without any load protection immediately postoperatively. On the other hand, uncemented prostheses, although requiring a biological adhesion process to the bone, have achieved better long-term survival outcomes. While uncemented prostheses offer some advantages over cemented ones, such as reduced surgical time and lesser biological impact due to the absence of the cementation process, it is important to note that their osseointegration is mediated by the same mechanisms that facilitate fracture healing. Consequently, biologically high-risk local situations, such as irradiated bone, or systemic conditions (chemotherapy aftermath) or other medications that

slow cellular turnover, are exposed to the risk of delayed osteointegration of the implant. Another contraindication to uncemented prostheses is severe osteopenia (Dorr C) due to the high risk of intraoperative fractures (see chapter on hip prosthesis complications).
Although the choice between cemented and uncemented implants remains tied to a comprehensive clinical evaluation and the preferences of the surgeon, the preferential indication for uncemented implants can be considered in young patients with higher functional demands and longer life expectations, and good bone quality.

CEMENTED HIP PROSTHESES

In cemented hip prostheses, the femoral and acetabular implants are slightly smaller in size compared to the osseous site where they are to be implanted. This is because the primary stability of the implant is entrusted to a layer of acrylic cement (PMMA) between the prosthesis and the bone; this can be employed for both the acetabular and femoral components or a hybrid fixation implant can be performed (only one cemented component). Acrylic cement was developed in the early 20th century in the aeronautical field. Its biocompatibility characteristics were accidentally discovered during the Second World War and were initially used in dentistry until the 1950s when the English orthopedic surgeon John Charnley first used it for cementing an orthopedic prosthesis at the hip level. This insight revolutionized prosthetic surgery, providing a reliable fixation methodology between the prosthesis and bone, and presenting itself as an alternative to uncemented implants, which at the time due to deficiencies in prosthetic design, limited availability of sizes, and non-biocompatible materials, were associated with a high rate of mobilization.
The introduction of cementation enabled immediate, reliable, and reproducible fixation, paving the way for the widespread dissemination of orthopedic prosthetic implants. Since then, numerous types and designs of implants have been proposed and used, and cementation of both acetabular and femoral components remains a valid and widely used option with short- and medium-term satisfactory results that justify its use.

Acrylic Cement in Orthopedic Surgery

Acrylic cement is constituted by two primary components: polymethyl methacrylate (PMMA) powder and a liquid catalyst, which includes a radiopaque agent for radiographic identification. Recent market offerings also include antibiotic-infused cements; prevalent formulations comprise either 1 gram of clindamycin and 1 gram of gentamicin per 50 grams of cement, or 1 gram of vancomycin and 1 gram of gentamicin per 50 grams of cement. Upon mixing these primary components, polymerization initiates. Initially, the cement displays a viscous liquid consistency, which facilitates its injection into a bony cavity. Within minutes, it attains a malleable state, ultimately reaching full hardness in approximately 12 to 15 minutes through an exothermic reaction.
The polymerization process can reach temperatures upwards of 100°C, leading to a slight expansion in volume, thereby enhancing the cement's osteo-implant gap-filling capabilities. However, this elevated temperature introduces the risk of cellular necrosis in adjacent osseous tissue. Furthermore, it presents a non-negligible risk (with an intraoperative mortality incidence of 0.11%, 95% CI: 0.07–0.15) of post-cementation embolism. The estimated mortality rate for cemented and non-cemented hip prostheses is 2.3% and 1.6%, respectively, although the generally older patient population for cemented prostheses may contribute to the higher mortality rate.
In addition to increased mortality, the bone cement implantation syndrome (BCIS) is characterized by hypoxia, hypotension, and/or unexpected loss of consciousness during the cementation period, prosthesis insertion, and joint reduction. The etiology and

pathophysiology of BCIS remain incompletely understood. Various mechanisms have been proposed, including monomer release into the bloodstream during cementation, embolism formation during cementation and prosthesis insertion, histamine release, complement activation, and vasodilation mediated by endogenous cannabinoids. Embolism usually occurs due to elevated intramedullary pressures during the cementation and prosthesis insertion processes. The cement undergoes an exothermic reaction and expands between the prosthesis and the bone, trapping air and medullary cells, and forcing them into the bloodstream.

Mechanically, the cement functions by filling the cavities in the cancellous bone, thereby creating a 'mold' effect that leads to gap-filling, rather than adhesive fixation (Figure: Cemented Prosthesis). Besides fixation, the cement serves the purpose of transmitting mechanical forces to the bone-prosthesis interface. Mechanical forces acting on the cement mantle are particularly complex in hip prostheses, as they are the summation of various stresses combined in bending, tension, shear, and torsion. Laboratory simulation of this complex situation is highly challenging; thus, to determine the cement's compressive and bending strength as well as its elastic modulus (or Young's modulus), strength tests have been simplified to two potential scenarios, i.e., in compression and in four-point bending, using both static and dynamic stresses. According to ISO standards (ISO5833), the minimum compressive strength requirement is 70 MPa. All commercial cements meet this criterion, with no significant difference in compressive strength between regular and antibiotic-added cements. The same ISO standard prescribes a minimum bending strength of 50 MPa and a minimum elastic modulus of 1800 MPa. Once again, all commercial cements meet these requirements, and the addition of antibiotics causes a reduction in bending strength, but not significantly so.

Cementation in orthopedic surgery offers the distinct advantage of providing immediate primary stability to the implant. This enables the implant to tolerate full loading without any restrictions. Additionally, the use of cement eliminates the need for specific sizing of the acetabulum and femoral canal, as the cement does not require bone interference for stabilization. Consequently, this minimizes the risk of intraoperative fractures, particularly in osteoporotic bone, and reduces the variety of implant sizes that need to be kept readily available.

Economically, cementation is a cost-effective technique. Furthermore, it exhibits a high medium-to-long-term survival rate (up to 15 years), which, in many cases, is reported to be equal to or greater than that of non-cemented fixation. However, a limitation compared to non-cemented implants lies in the higher rate of long-term loosening (20 years), especially concerning the acetabular component.

Uncemented Hip Prostheses

In the setting of uncemented hip prostheses, both the femoral and acetabular components are slightly oversized relative to the corresponding osseous sites to achieve primary stability via "press-fit." This entails close contact between the bone and the implant. Secondary stability is achieved biologically through osseointegration over a period of 4-8 weeks, dependent on the bone quality, material of the implant, and the level of primary stability attained during the surgical procedure. Uncemented fixation can be used for both components, or a hybrid implant can be employed, which utilizes a non-cemented acetabular cup and a cemented stem.

Although uncemented implants were developed prior to their cemented counterparts, early outcomes were unsatisfactory. Numerous failures were attributed to inadequate prosthetic design and smooth surfaces, which were unable to achieve either primary or secondary

stability. A major milestone in the development of modern uncemented hip prostheses was set by Konstantin Mitrophanovich Sivash, who presented his results at a conference on osteoarticular tuberculosis in Moscow in 1963. His design featured a titanium press-fit acetabulum, a non-cemented stem, and a cobalt-chromium (MoM) articulating couple. Unfortunately, geopolitical conditions at the time prevented the dissemination of his innovative ideas in the West for approximately 15 years.
In the Western context, the concept of biological fixation, or osseointegration, was first introduced by Robert Judet in 1971, who proposed a prosthesis with a highly porous "porometal" surface composed of a chromium-cobalt-nickel-molybdenum alloy. By the mid-1980s, a biomaterials research group from Leiden, Netherlands, led by Prof. Geesink, along with Prof. Furlong of London, Dr. Manley of Osteonics, and Prof. Epinette of Bruay-Labuissiere, France, had introduced the use of a bioactive coating for secondary implant integration—hydroxyapatite. Prof. Lord's concept that "living bone, undergoing remodeling, ensures stable implant fixation" was foundational to this innovation.
Since then, continual advancements have been made both in prosthetic design and materials. These advances have made the application of uncemented implants a reliable and reproducible procedure with encouraging long-term outcomes. This scientific treatise aims to provide an in-depth understanding of the development, mechanisms, and clinical applications of uncemented hip prostheses, grounded in historical background and current evidence-based practices.

Materials Employed in Articular Coupling: A Comprehensive Review

Polyethylene

It was Sir John Charnley who, in the 1960s, pioneered the use of high molecular weight polyethylene (HMWPE) in hip replacement to construct the acetabular component. Polyethylene is a semicrystalline polymer of ethylene, specifically organized in a reticular pattern when utilized in orthopedic applications. The high molecular weight enhances both wear and impact resistance without sacrificing ductility. Initial implementations of this material displayed unsatisfactory long-term wear rates, which led to the introduction of cross-linked polyethylene in the 1990s. This newer form underwent irradiation processes to induce new interchain bonds, offering increased wear resistance but greater susceptibility to oxidation, resulting in the deterioration of its tribological characteristics over extended periods. Further evolution in the 2000s saw the introduction of Vitamin E as an antioxidant to augment long-term wear resistance further. The material's ductility and mechanical strength have enabled the design of raised edges (anti-dislocation rims) or retentive head mechanisms to minimize dislocation risks. Polyethylene remains the most globally employed material for acetabular liners and, in its latest formulations when paired with ceramic heads, has shown excellent long-term survival rates. The initial drawbacks, such as premature aseptic mobilizations from osteolysis due to wear debris, have been largely overcome. The singular limitation of modern polyethylene is its elevated wear rate compared to ceramic when used with larger diameter heads.

Metal

In the context of metallic components in articular coupling, reference is typically made to articular surfaces composed of a crystalline alloy of Chromium-Cobalt-Molybdenum (CrCoMo), characterized by high mechanical strength and resistance to corrosion and wear. These metallic components can either be utilized solely at the femoral head to form a metal-on-polyethylene (MOP) coupling or at the acetabular liner level to create metal-on-metal (MOM) pairings.

The effective functioning of metallic articular surfaces is contingent on their self-lubricating capabilities. Usually, the thickness of the surface lubricating film exceeds the asperities of the metal surface by a factor proportionally related to the dimensions of the cup and head as well as the radial clearance. Thus, a high radius value of the head (large diameter head) coupled with low radial clearance facilitates the dragging of lubricant into a gradually converging space between the surfaces, thereby reducing polar stress. Conversely, small head sizes, erroneous component placements, and an increase in radial clearance can compromise the fluid film dimensions. It is believed that acetabular inclination angles greater than 50 degrees and extreme combined anteversions are negative predictive factors, inducing material wear and the subsequent release of debris and ions.
The allure of metal-on-metal (MoM) articular coupling has consistently resided in its ability to offer younger and active patients low wear rates in combination with large-diameter heads, bordering on anatomical reconstruction. Despite this, MoM implants are not without complications. Notably, several such devices have been withdrawn from the market due to unacceptable medium-term failure rates, prompting some manufacturers to impose restrictions on indications. Specifically, total hip arthroplasties employing MoM couplings have demonstrated suboptimal long-term results due to wear at the neck-head interface (known as "trunnionosis") and cases of inflammatory reactions arising from metal wear (termed "metallosis"), resulting in both local and systemic ion-induced damage.
All MoM joints are subject to wear from dynamic loading and corrosion from biological fluids, synergistically resulting in a phenomenon known as tribocorrosion. Normally, metal corrosion resistance is maintained by the continuous repassivation of surfaces, facilitated by the presence of body fluids. When this repassivation layer is disrupted due to excessive pressure between surfaces, friction occurs, leading to progressive wear and the release of metal ions and toxic debris into surrounding tissues. These debris particles further exacerbate the situation by causing additional surface damage through foreign body abrasive wear.
The risks associated with surface wear and adverse reactions to metallic ions have reduced the viable indications for the use of MoM couplings. Such utilization is no longer justifiable in light of the excellent outcomes and reduced complications guaranteed by other coupling mechanisms. The use of MoM coupling now remains a limited indication for select cases involving resurfacing implants. Although these implants come with specific issues related to their unique design, they are less susceptible to the surface-induced damage common to MoM and may be considered for younger, active patients. However, it should be noted that female gender and femoral resurfacing heads smaller than 50 mm are correlated with higher failure rates.

Ceramic

Since 2005, the ceramic material employed for articular couplings in orthopedics is primarily composed of alumina oxide reinforced by zirconia. This formulation enhances the material's hardness and hydrothermal stability. Ceramics are known for their excellent tribological properties, combined with high biocompatibility, but they are also characterized by fragility when subjected to repeated microtrauma—a limitation particularly relevant to older generation ceramics with a low zirconia content.
New-generation ceramics have demonstrated excellent 15-year survival rates, even in younger patients, with robust clinical and radiographic outcomes. Osteolysis is largely anecdotal in the context of ceramic couplings. The wear debris of ceramics is biologically inert and well-tolerated, inducing only minimal granulomatous response. Given their outstanding tribological attributes, ceramic femoral heads have become the gold standard in Western countries, replacing metal heads.

Nevertheless, ceramics are not without specific complications that must be recognized and considered (see related chapter). Component fracture is a rare but potential complication, most often occurring suddenly and acutely. Most such events are of traumatic or iatrogenic origin, due to imperfect surgical techniques. Noise represents another typical ceramic-related complication. This can manifest as a squeaking or clicking sound, evoked by certain hip movements, and may become frequent and intense enough to cause patient concern and discomfort. The genesis of this noise remains poorly defined but is likely the result of imperfect surface lubrication under load. Noise is more common in male, young, active, and overweight patients, as well as in those with anteverted acetabular components and suboptimal positioning. Although not a pathological condition per se, this complication is associated with an increased risk of component breakage, typically occurring within five years of noise onset, which serves in this instance as a prodromal symptom. Suboptimal positioning is also correlated with premature ceramic wear, known as stripe wear. This phenomenon is related to component micro-instability arising from incorrect soft tissue tensioning or imprecise positioning (excessive acetabular abduction and/or extreme combined anteversion). In essence, these predisposing conditions cause the components to articulate over short surface segments, resulting in localized overload and subsequent wear.

Surgical Approaches

Multiple surgical approaches have been developed for the execution of hip replacement, each with its specific advantages and disadvantages. The most commonly employed surgical pathways for hip replacement include the posterolateral approach, the direct lateral approach, and the direct anterior approach. Over the years, and with the advent of novel surgical instruments, each of these approaches has undergone modifications in an attempt to minimize invasiveness, thus reducing biological damage to the patient and facilitating early rehabilitation.

The posterolateral approach, also known as the Southern or Moore approach, aims to access the articular plane from the posterior, by spreading the distal fibers of the gluteus maximus muscle and dissecting the external rotator muscles (piriformis, superior and inferior gemellus, external and internal obturator, and quadratus femoris), followed by posterior hip dislocation. This access provides good visualization of the posterior capsule and the entire acetabulum, although managing fractures of the anterior acetabular wall may be challenging. Femoral exposure is straightforward, facilitating good visualization of the lesser trochanter, an important intraoperative landmark.

The primary advantages of this approach include the sparing of abductor musculature, with resultant biomechanical benefits, ease of distal extension of the surgical route in case of femoral intraoperative complications, reduced incidence of heterotopic ossifications compared to the lateral approach (due to sparing of the abductor muscles), relative simplicity of the surgical technique, and rapidity of execution. The main disadvantage lies in the necessity to perform the surgery with the patient in the lateral decubitus position, which results in the loss of key anatomical landmarks that can be assessed in the supine position, leading to difficulties in positioning the acetabular component, especially in terms of anteversion, and in intraoperative limb-length assessment. The most vulnerable structure in this approach is the sciatic nerve, due to its relationship with the piriformis muscle.

The principal complication associated with this approach, in comparison to others, is post-operative dislocation, generally posterior, due to weakening of the containment structures (articular capsule, external rotators) of the posterior wall. Minimizing this risk necessitates meticulous reconstruction of the posterior capsule and the short external rotator musculature, particularly the piriformis tendon.

The direct lateral approach, also known as the Hardinge or Charnley approach, allows access to the articular plane by partially detaching the medius and minimus glutei from their insertion on the greater trochanter, followed by anterior femoral dislocation. The patient can be positioned either in lateral or supine decubitus; the latter is usually preferable for superior visualization of anatomical landmarks to be used during the procedure.
Advantages include excellent exposure of both the acetabulum and femur, easy extension of the surgical route at both the proximal and distal levels, and sparing of posterior containment structures of the hip (reduction in post-operative dislocation rates). Additionally, major vascular and neural structures are relatively distant from the surgical field (except for the inferior gluteal artery, which must be preserved in case of proximal extension of the incision). However, the necessity to partially detach the minimus and medius glutei from the greater trochanter compromises the abductor and antigravity function of these muscles, leading to post-operative limp (termed gluteal limp) and a positive Trendelenburg sign, reported in the literature in up to 10% of cases. This is also the surgical approach with the highest incidence of heterotopic ossifications, mainly due to the abductor musculature's tendency to calcify in response to surgical stress.
To minimize the risk of gluteal insufficiency, it is imperative to perform a meticulous suture of the medius gluteus tendon, ensuring its continuity and that the suture guarantees good strength. In the initial post-operative weeks, patients are prescribed a rehabilitation protocol that includes partial weight-bearing on the operated limb to allow tendon healing.
The direct anterior approach, also known as the Smith-Petersen or Heuter approach, has regained popularity among surgeons in recent years for prosthetic replacements as well. This surgical access exploits the intermuscular interval between the tensor fasciae latae and the sartorius muscle, thus allowing the articular plane to be reached and the arthroplasty to be performed without detaching any muscle. The main vascular and neural structure at risk with this approach is a sensory nerve, the lateral femoral cutaneous nerve.
The main advantages of this approach include excellent visualization of the acetabulum, reduced bleeding, and reduced post-operative pain, facilitating early rehabilitation. The major limitation is the challenging exposure of the femur, which increases the risk for intraoperative fractures. Moreover, this approach requires a more complex distal extension than the others, necessitating a greater learning curve and the utility of specialized instruments and limb positioning tables.

Rehabilitation and Recovery Timeframes Following Total Hip Replacement

Achieving an excellent clinical outcome following THR requires an optimal postoperative rehabilitation program. The program should be individualized, taking into consideration preoperative activity levels, postoperative expectations, preoperative anatomical anomalies, surgical approach employed, prosthesis components, and any intraoperative or perioperative complications. Advances in surgical techniques, minimally invasive approaches, and improved pain management protocols have facilitated increasingly accelerated rehabilitation timelines. Anesthesia and pain control techniques should be aligned with postoperative functional recovery goals.
The rehabilitation program can be divided into three phases:

- Preoperative Phase: This phase involves educating the patient about recovery timeframes, rehabilitation modalities, and potential implant-related complications and their prevention. It may also be beneficial to instruct the patient on using crutches and gait patterns with assistive devices.
- Immediate Postoperative Phase: Commencing immediately after the return of voluntary motor function, this phase includes isometric exercises (active knee extension) and antithromboembolic exercises (ankle dorsiflexion and plantar flexion). These exercises can be performed autonomously while in bed. Under the guidance

of a physiotherapist, the patient may also be mobilized, be made to assume a sitting and even standing position on the same day as part of an intensive rehabilitation program. Alternatively, these activities can be delayed to the subsequent days (first and second postoperative days). Pain management, improving patient autonomy, initiating muscle strengthening exercises, achieving a joint range of motion between 0° and 80°, and introducing partial weight-bearing ambulation with forearm crutches are crucial during this phase. Contractures causing apparent limb length discrepancies should be corrected. The patient should also be educated about movements that risk dislocation, with precautions tailored to the specific surgical approach. For all approaches, adduction is generally avoided, but specific caution against hyperextension-external rotation is advised for anterior approaches, whereas flexion-external rotation is avoided in direct lateral approaches. For posterolateral approaches, flexion-internal rotation is discouraged. The patient can be considered for discharge when clinically stable, able to walk independently with crutches over short distances, ascend and descend stairs with aids, and perform self-care tasks.

- Post-discharge Phase: The physiotherapy program should include a gradual increase in joint range of motion up to 90°, muscle strengthening exercises focusing on abductors, flexors, and extensors, stretching of the adductor muscles, and optimization of ambulation with crutches. Once a balanced pelvic gait is achieved, ambulation without crutches may be permitted for extended distances. Subsequently, exercises to further strengthen muscles, increase joint range, and optimize gait should be encouraged. Water-based exercises, cycling with gradual saddle lowering, independent ambulation, and resistance exercises targeting abductors are beneficial. Complete recovery typically occurs around 40 days post-surgery. Anti-dislocation precautions can generally be lifted 25 days post-surgery with soft tissues adequately healed. However, patients must continue to avoid extreme movements that pose a risk of dislocation or impingement and maintain sufficient muscle strength, particularly focusing on abductor muscle trophism.

Postoperative Assessment of a Hip Prosthesis

The postoperative evaluations of a hip prosthesis are tailored to the individual patient's specific characteristics and those of the implant. As best practice, an initial assessment should be conducted within 20-30 days, followed by additional evaluations at 3-6 months, 12-18 months, and subsequently biennially. It is advisable to maintain a high level of vigilance during the first 1-2 months to identify and treat potential early complications (infections, early dislocations). Subsequent assessments should focus on monitoring osteointegration around 6-12 months to identify early mobilizations, typically occurring within the first two years. As time progresses, the frequency of follow-up visits may be lengthened, although periodic clinical and radiographic evaluations should never be entirely discontinued.

The follow-up assessments consist of a clinical evaluation combined with recent anteroposterior and axial radiographs of the operated hip. Clinical assessment aims to verify the presence of newly emerged pain or limping, the condition of the skin around the scar, painless passive mobilization of the hip in flexion rotation, and active mobilization with a focus on active flexion and abduction. Particular attention should be given to autonomous ambulation, specifically to pelvic obliquity, gluteal insufficiency limp, or escape limping.

Radiographic evaluation is critically important since some complications, such as polyethylene wear or adverse metal reactions, may manifest as early radiographic anomalies in asymptomatic or minimally symptomatic patients. Radiographic assessment should be compared to the initial postoperative radiograph and all subsequent radiographs. Reviewing the preoperative radiograph may also provide insights into surgical choices,

residual leg length discrepancies, and the accuracy of biomechanical parameter reconstruction.
In postoperative radiographs, attention must be directed to the centering of the head, movement of the prosthetic components compared to immediate postoperative radiographic control (movement is unequivocally a sign of prosthesis failure termed "mobilization"), osteolysis, radiolucent lines, and periosteal reactions. These signs could indicate dislocations, wear, aseptic or septic failures.
On the acetabular side, a well-integrated cup shows the absence of radiolucent lines, radial bony trabeculae, superolateral and inferomedial buttresses, and medial areas of bone rarefaction (stress shielding). Mobilized acetabular components demonstrate progressive movement (rising or rotating) of more than 2 mm in two consecutive radiographs. Moreover, radiolucent lines greater than 2 mm, circumferential to the acetabulum, are frequent.
On the femoral side, a well-integrated stem shows the absence of diffuse radiolucent lines and multiple radial trabeculae. No varus-valgus or sinking mobilizations relative to a fixed point should be evident. A certain degree of sinking may be immediately evident postoperatively; however, it must be clinically contextualized and should progress to stabilization in subsequent assessments. Differentiated diagnoses (primarily infection) should not be neglected. For cemented stems, the uniformity of cementation, absence of radiolucent lines at the prosthesis-cement interface, and absence of cement mantle fractures must be evaluated.
Articular surfaces should be scrutinized carefully. Polyethylene liners undergo normal wear, manifesting as an eccentric femoral head and liner thickness reduction in the superolateral quadrant compared to the inferomedial quadrant. They often accompany periprosthetic osteolysis and changes in the shape of soft tissues (foreign body reactions, see complications). Similarly, metal-on-metal surfaces, which show no gross signs at the joint level, may accompany periprosthetic osteolysis and pseudotumors. Failures in ceramic-ceramic pairings can result in the release of radiopaque intracapsular particles and liner malpositioning relative to the acetabular cup.
Radiographic anomalies must always be clinically contextualized, compared to subsequent radiographic controls, and further investigated through secondary-level tests.

COMPLICATIONS

Total hip replacement demonstrates exceedingly high success rates; complications are relatively rare. However, due to the increasing prevalence of prosthetic replacements, complications are becoming a progressively more significant issue. Complications can be general in nature, arising as a consequence of major surgical intervention (see medical and anesthetic complications of surgery), or they can specifically pertain to total hip replacement. They can be categorized as intraoperative and postoperative, with the latter further subdivided into early and late complications.

Unstable Hip Prosthesis: Diagnosis and Treatment

Instability is defined as the temporary and incomplete loss of articular contact between prosthetic components, with variable but generally benign clinical outcomes. In contrast, dislocation refers to a clinically significant event characterized by the complete loss of articular contact between the femoral head and the acetabular cup.
These complications represent a major cause of implant failure, with an incidence reported in the literature of up to 5%, particularly during the first postoperative year. Key risk factors for instability and dislocation include female sex, advanced age, neuromuscular disorders, abductor muscle insufficiency, and alcohol abuse. The dislocation can be either posterior or anterior, based on the position of the femoral head relative to the acetabular cup. Posterior dislocation typically occurs following a posterior-lateral approach due to hip flexion,

adduction, and internal rotation; whereas anterior dislocation can follow an anterior approach due to hyperextension, adduction, and external rotation.
The etiological factors for dislocation may involve malpositioning of the prosthetic components (see combined anteversion), inadequate function and tension of periarticular muscles, lack of patient cooperation during the immediate postoperative period, excessive wear of the acetabular liner (polyethylene), or its breakage (ceramic). The incidence of prosthetic dislocation is higher during the first 60 postoperative days due to reduced muscle tone and/or the pathway created by the surgical approach, which generates a zone of lesser resistance not adequately protective against dislocation. In subsequent weeks and months, a scar tissue capsule forms around the prosthetic implant, limiting extreme joint movements and providing adequate protection against potential dislocation (Figure 14.265). Late dislocation (beyond 90 days) usually occurs due to excessive motion, post-traumatic events (sprains, falls), or polyethylene wear.
Clinical presentation of unstable hip is typically insidious; upon physical examination, patients may report a sensation of snapping or internal movement within the hip, a feeling of discomfort at extreme ranges of motion, sometimes accompanied by pain or a sense of apprehension. Clinical manifestations of hip prosthesis dislocation are more apparent; patients typically present in an emergency setting in a supine position, with severe pain, complete functional impairment of the limb, and extreme pain upon any attempt at movement. Peripheral neurological examination is essential, testing active and passive ankle and foot movements, and a valid quadriceps muscle contraction to identify potential sciatic or femoral nerve involvement. Anamnestic data collection is crucial, including any previous dislocations or instabilities, and the reconstruction of the event that led to the dislocation.
Initial assessment should include a thorough history; documenting the timing of the surgical procedure, the surgical approach used, the type of prosthetic model, the postoperative course, and any prior dislocations or subluxations. The patient should be queried regarding any comorbidities (neuromuscular disorders) and previous treatments (surgical interventions, medical therapies). Radiographic evaluation is indispensable; conventional radiography allows, within certain limitations, for the estimation of implant position and orientation, and any wear of the polyethylene liner. However, dislocation usually occurs predominantly due to incorrect combined positioning of the acetabulum and femur on the axial plane (combined anteversion of the femur and acetabulum), necessitating CT scans for precise measurement of these parameters.
Early dislocation (within the first month post-implantation) can be effectively managed conservatively with strict functional limitations and anti-dislocation devices maintained for six weeks, the time needed for soft tissue healing around the prosthesis. When conservative measures fail to achieve a stable implant or non-surgical treatment fails, surgical intervention is warranted. The goal of revision surgery is to replace the malpositioned prosthesis with components adequately oriented. Combined anteversion should be a minimum of 30º and not exceed 50º. When the dislocating condition is not solely attributable to prosthetic malpositioning but has a multifactorial etiology, primarily muscular, alternative surgical strategies should be employed, involving special acetabular components (dual-mobility cups); larger prosthetic heads (increased jump-distance); anti-dislocation liners (Figure 14.266) properly oriented to protect against dislocation; distalization of the greater trochanter or lateralized prosthetic stems (with increased offset to amplify joint reaction forces by placing periarticular muscles under appropriate tension); retentive components (that lock the prosthetic head within the acetabulum); and muscle plastic surgery (reconstruction of the abductor musculature).

The treatment strategy must be predicated upon the accurate etiological characterization of the instability. The table presents the primary parameters potentially responsible for the instability and dislocation of the implant. (TABLE 1)

Type of Instability	**Acetabular Orientation**	**Stem Orientation**	**Abductor Mechanism**	**Impingement**	**Wear**	**Recommended Type of Revision**
Acetabular Malpositioning	Incorrect	Correct	Intact	Absent	Absent	Revision of the Acetabulum
Malposizionamento stelo	Correct	Incorrect	Intact	Absent	Absent	Isolated Revision of the Stem
Deficienza abduttoria	Correct	Correct	Damaged	Absent	Absent	Repair of the Abductor Complex. Incorporate Dual Mobility or Retentive Acetabulum
Impingement	Correct	Correct	Intact	Present	Absent	Remove the Cause of Impingement, Dual Mobility Acetabulum or Revision of Modular Parts
wear	Correct	Correct	Intact	Absent	Present	Revision of the liner or the Acetabulum
Causa sconosciuta	Correct	Correct	Intact	Absent	Absent	Dual Mobility, Retentive Acetabulum

Table 1: Parameters of Instability and Implant Dislocation

TOTAL HIP REPLACEMENT IN PATIENTS WITH ALTERED VERSION AND PELVIC KINEMATICS

Regardless of its documented efficacy, Total Hip Replacement (THR) is accompanied by a certain rate of failure, which subsequently necessitates revision surgeries. As the prevalence of THR is projected to escalate in the coming decades, a concomitant rise in the demand for revision surgeries is anticipated. Complications tend to be higher in specific patient subgroups, notably those with a pre-existing history of lumbar spine disorders or patients subjected to LS surgeries, who may manifest pathological changes in pelvic version and kinematics.

At present, owing to advancements in prosthetic implant technology that incorporate tribological principles into material engineering and design, the incidence of dislocation largely hinges on the interdependent relationship between the implant components (combined anteversion) and the overall overall body balance.

Combined anteversion poses limits to cup and femoral anteversion to decrease the risk of impingement and dislocation[6]. Conversely, body balance is impacted by the interplay between the spine and pelvis, recently termed as "spinopelvic balance." When this balance is aberrant, patients exhibit abnormal pelvic anteversion in both standing and sitting positions. This places THR at risk for impingement due to mechanical conflicts—either between two prosthetic components, between bone segments, or between a bone segment and a prosthetic component. Such impingement can generate a levering effect, leading to accelerated wear and an increased risk of implant dislocation.

In 1978, Lewinnek et al. proposed a "safe zone" for the positioning of the cup in THR implants as a means to mitigate the risk of impingement and dislocation[5]. Subsequent research, however, indicated that dislocations still occurred in THRs that were placed within this purported safe zone. The limitation lies in the conceptualization of the safe zone as a "static value," which only partially reflects reality. This is because alterations in pelvic version on the sagittal plane, often secondary to spinal pathologies, influence the orientation of the acetabulum when transitioning from a standing to a sitting position. The hip is predominantly affected by the lumbar vertebrae; as such, the complex relationship between the spine, pelvis, and hip can be adequately assessed through a lateral radiograph encompassing the L1-3 vertebrae to the proximal part of the femur[7–12].

Spino pelvic balance and alignment

Spinopelvic balance is a multifaceted mechanism influenced by both spinopelvic version and kinematics. Notably, a significant aspect of human balance is afforded by mobility in the sagittal plane, where flexion and extension movements are collaboratively orchestrated between the lumbar spine and pelvis, creating a unique biomechanical interplay. When the spine's contribution to this coordinated movement is compromised or absent due to rigidity, the hip and pelvis are necessitated to augment their range of movement to facilitate activities of daily living. Another critical scenario arises from an aberrant positioning of the pelvis in the sagittal plane, which could manifest as a pathologically fixed retroversion or, less commonly, anteversion. This misalignment disrupts the synchronized movement between the spinopelvic complex and the hip. In either case, aberrant motion in THR may precipitate prosthetic impingement and, potentially, lead to implant dislocation[13,14].

Spinal mobility can be compromised due to conditions such as degenerative or developmental diseases, or subsequent to spinal fusion surgery. Over the past decade, spinal fusion or inherent spinal stiffness has been increasingly observed in patients who are candidates for THR. When examining the annual epidemiology of THRs, with approximately 330,000 performed in the United States and around 59,000 in Italy, roughly 1% are executed on patients with a rigid or fused lumbar spine (LSF). Multiple studies have indicated an elevated risk of mechanical complications in THR implants among the population who have undergone surgical procedures for LSF. This risk is attributed to the partial disruption of spinopelvic kinematics that strains compensatory mechanisms to their limit. This clinical observation has catalyzed research focusing on the hip-spine relationship, providing orthopedic surgeons with the requisite knowledge and tools to properly manage THR patients affected by lumbar spine conditions. In these investigations, patients who underwent surgery for LSF displayed a higher incidence of long-term mechanical failure; such an outcome was not observed in patients who underwent non-fusion surgical interventions. Additionally, it was found that failures in THR implants among those with prior fusion surgeries tended to manifest within the first two years following the THR procedure. This underscores the critical importance of comprehensive implant positioning and patient alignment in mitigating implant-related complications[15–18].
Under normal physiological conditions, the spinal column exhibits a straight configuration in the frontal plane and possesses four distinct curves in the sagittal plane: two anterior convexities situated at the cervical and lumbar regions, termed lordosis, and two posterior convexities located at the thoracic and sacral regions, designated as kyphosis. There exist no universally accepted standard values for sagittal curvatures in the adult spine. However, thoracic kyphosis (TK) typically varies between 20° and 45°, while lumbar lordosis (LL) predominantly falls within the 30° to 60° range. This lack of standardized values stems from the primary function of the spinal column, which is to sustain an upright posture with minimal energy expenditure. Furthermore, LL is intrinsically linked to the width of the pelvis, quantitatively expressed by the angle of pelvic incidence, as well as pathological conditions affecting the lumbosacral junction, such as spondylolisthesis. Irrespective of individual curve magnitudes, a balanced spine ensures global compensation by aligning the center of gravity between the centroid of the last cervical vertebra's body and the sacrum, commonly referred to as the Sagittal Vertical Axis (SVA). The sagittal curves of the spine facilitate the maintenance of equilibrium and even weight distribution by channeling the load from the spine through the lower extremities to the ground. Hence, the comprehensive assessment of inter-segmental relationships within the spinal column and between the lumbar spine and pelvis holds greater clinical relevance than the numerical quantification of individual angles for evaluating sagittal vertebral balance.
Evaluation necessitates the measurement of specific radiographic parameters viewed sagittally across the entire spine and pelvis, such as Pelvic Incidence (PI), Sacral Slope (SS), Pelvic Tilt (PT), Acetabular Anteversion (AA), and Anterior Pelvic Plane (APP). Pelvic Incidence (PI) is an angle formed by a line perpendicular to the S1 endplate and a second line extending from the midpoint of S1 to the center of the bicoxofemoral axis. The PI value reflects the pelvis's capacity to compensate for sagittal spinal imbalance through rotation around the bicoxofemoral axis. A higher PI suggests a greater potential for pelvic

retroversion. It is equivalent to the sum of SS and PT, which explains the inverse relationship between SS and PT.

Sacral Slope (SS) is an angle created between the S1 endplate and a horizontal line. Elevated SS values indicate a horizontally oriented sacrum (anteverted pelvis), whereas negative values make standing difficult.

Pelvic Tilt (PT) is an angle formed by a line from the midpoint of the S1 endplate to the center of the space between the two femoral heads and a vertical line. It signifies the spatial orientation of the pelvis, which can change depending on the patient's standing and walking posture. It is complementary to SS; as the pelvis rotates backward (retroversion), PT increases, and it decreases when the pelvis rotates forward (anteversion).

Acetabular Anteversion (AA) is an angle created by a line along the long axis of the acetabulum and a horizontal line measured on sagittal radiographs.

Anterior Pelvic Plane (APP) is a plane formed by the anterior-superior iliac spines (ASIS) and the pubic symphysis. In a neutral spinal balance, this plane corresponds to the Functional Pelvic Plane (FPP), a vertical plane through the pubic symphysis and ASIS, perpendicular to the ground.

Sagittal Vertical Axis (SVA) represents the horizontal distance between a plumb line originating from the body of C7 and extending perpendicularly to the ground and the posterosuperior angle of S1. This parameter describes the overall sagittal balance of the thoracolumbar spine and is considered normal within 5 cm. Values between 5 and 15 cm indicate partial compensation, while alignment is considered decompensated when the measurement exceeds 15 cm.

Intricate relationships exist among these aforementioned parameters. Foundational guidelines for sagittal spinopelvic balance have been provided by Le Huec and Hasegawa, defining the equations $PI = PT + SS$ and $PT = 0.44\ PI - 11°$. Additionally, the most commonly employed equations to delineate the relationship between LL and PI are those formulated by Schwab: $PI = LL \pm 11°$, and Le Huec: $LL = 0.54 \times PI + 27.6°$ [19–22].

In individuals possessing normal spinopelvic flexibility, the pelvis exhibits a posterior tilt when transitioning from an upright standing position to a seated posture. This posterior tilting of the pelvis synchronously induces a posterior tilt of the acetabulum, thereby providing sufficient space for the femur to flex towards the acetabulum. Intriguingly, each degree of posterior pelvic tilt (PT) correlates with a nearly equivalent one-degree increase in the anteversion of the acetabulum. This relationship allows the femur to achieve maximum flexion towards the acetabulum without the risk of impingement.

The standard range of motion typically involves a posterior pelvic tilt ranging from 20° to 35° and femoral flexion extending between 55° to 70° relative to the acetabulum. This coordinated motion culminates in an angle of approximately 90° between the femur and the upper body, thereby facilitating an erect sitting posture. However, with diminished pelvic mobility, compensatory mechanisms are activated in the femur to increase its range of motion to accommodate necessary postural alterations. Specifically, a decline in spinopelvic mobility is associated with a proportional escalation in the degree of femoral flexion required to achieve an upright sitting position. To elaborate, for each degree of lost pelvic motion, an increase of approximately 1° in femoral flexion becomes necessary to allow both the femur and the upper body to attain the intended upright posture[4,7,23–29].

Quantification of spinopelvic motion, hip movement, acetabular positioning, and femoral range of motion can be achieved through the radiographic measurement of these parameters using lateral views of the lumbar spine and pelvis. This involves calculating the

differences between two distinct postural positions, namely standing and sitting. Nonetheless, this method is not without limitations. First, despite any pelvic twisting, the radiographic images must conform to anatomical symmetry to prevent overlapping of landmarks, which would complicate image interpretation. Second, a sagittal view may not suffice for the functional evaluation of the so-called "safe zone."
Instability and dislocation in LS patients are believed to be related to inadequate positioning of the acetabular cup and femoral stem, as demonstrated by a study of full 3D functional-anatomy of the pelvis (using EOS technology)[30] pointing out the effect of pathological pelvic changes on the risk of impingement.

Concomitant LS surgeries

Patients with a history of lumbar spine procedure, whether performed before or after hip prosthesis replacement surgery, may exhibit a limitation in the movement of the lumbar spine and potentially present an altered pelvic alignment, as a consequence of corrective surgical strategy or in relation to mechanical failure of the construct and the development of compensatory mechanisms (failed back syndrome). Given the functional relationship between the hip and lumbar spine, surgical interventions in one anatomical region may influence the pathological trajectory of the other.
The demographic aging, broadening of clinical indications, advancements in minimally invasive surgical methodologies, as well as improvements in anesthesiological techniques that enhance patient eligibility for major surgical interventions, have collectively contributed to a heightened prevalence of individuals undergoing both THR and Lumbar Spine (LS) surgery within their lifetime.
Patients with spinopelvic fusion and total hip replacement present a 20% incidence of dislocation[3]. In a registry study[31], patients with spinal fusion and hip replacement found a dislocation incidence doubled when compared to the control group with only hip replacement.
Current literature primarily focuses on the elevated risk of complications in patients who have undergone lumbar spine fusion (LSF) procedures, where limitations in spinopelvic mobility and potential changes in pelvic version may adversely impact the functional coupling between the acetabular cup and prosthetic femoral head. Such disparities in "coupled anteversion" can engender limited range of motion, altered biomechanical dynamics, and decreased tolerance to suboptimal implant positioning, thereby contributing to a rise in mechanical complications in THR[5,6,32].
A recent European investigation corroborated an augmented frequency of mechanical complications in patients with concomitant THR and LSF, partially substantiating data from American databases[10,33]. Conversely, the repercussions of non-fusion lumbar spine surgical interventions on THR longevity remain sparsely explored.
Utilizing registry-based data, Eneqvist et al. revealed that a small but noteworthy percentage (3.5%) of THR patients had undergone lumbar spine surgery in the preceding 11 years, and these individuals generally manifested suboptimal THR outcomes[34]. The inquiry into the distinct impacts of lumbar spine fusion and non-fusion procedures on THR, as well as the reciprocal effects of THR on lumbar spine interventions necessitating subsequent revision, remains an under-researched domain.
A recent registry-based comparative study indicated that 2.2% of THR patients had previously undergone lumbar spine surgical procedures. Among these, less than half involved LSF. Survival analysis demonstrated superior THR implant longevity in patients without prior lumbar spine surgery, with those undergoing LSF manifesting an elevated risk of revision[35](Chart 1). Intriguingly, when mechanical complications were solely

considered as endpoints for THR survivorship, non-fusion lumbar spine surgery patients displayed superior implant survival relative to their fusion counterparts, particularly during the initial five-year postoperative period.
Also, approximately 80% of all mechanical failures (constituting nearly 70% of total failures) were notably concentrated within the first two years post-primary THR in patients with a history of lumbar spine surgical interventions. Concerning the likelihood of necessitating lumbar spine revision following THR, no significant disparities were discerned between fusion and non-fusion cohorts.
These data indicate superior THR implant longevity in non-fusion lumbar spine patients as compared to their fusion counterparts, especially when biomechanical complications necessitating revision surgeries are considered.

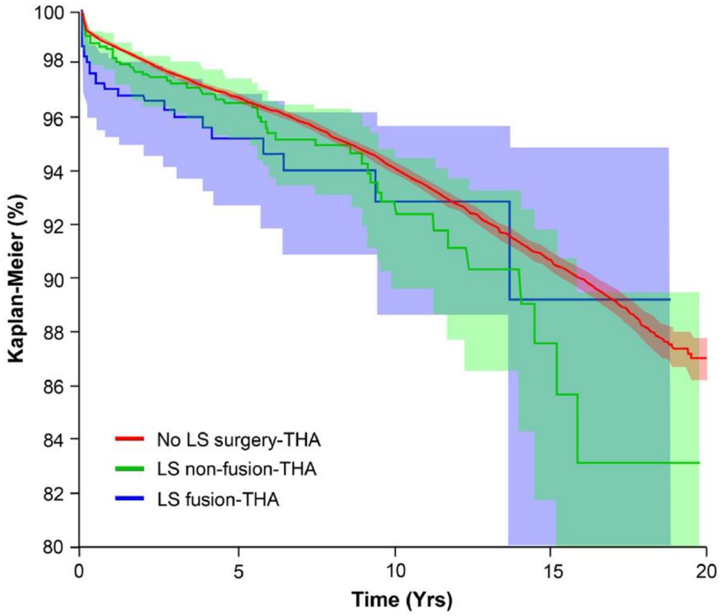

% Survivorship (95% confidence interval)							
	1Y	3Y	5Y	7Y	10 Y	13Y	15Y
Non-LSsurgery-THA	98.6 (98.5-98.7)	97.5 (97.4-97.7)	96.7 (96.6-96.9)	95.9 (95.7-96.0)	94.1 (93.9-94.3)	92.0 (91.7-92.3)	90.7 (90.3-91.0)
Prostheses at risk	71173	59438	48823	38842	25278	14114	8619
LS fusion-THA	96.8 (94.98-98.0)	95.7 (93.5-97.2)	94.6 (91.9-96.4)	94.0 (91.0-96.0)	92.9 (88.9-95.5)	92.9 (88.9-95.5)	88.7 (76.8-94.9)
Prostheses at risk	458	311	200	133	72	25	14
LS non-fusion-THA	98.2 (97.2-98.8)	96.8 (95.6-97.7)	96.1 (94.6-97.1)	94.8 (93.0-96.1)	91.9 (89.2-94.0)	90.6 (87.2-93.2)	87.7 (81.9-91.8)
Prostheses at risk	1070	846	632	445	232	97	45

Chart 1: Implant survival in THR versus THR and LS surgery patients. Dashed lines represent confidence intervals.

Multiple investigations corroborate the association between THR and preceding or succeeding LSF procedures[36–38]. There is a prevailing consensus to prioritize THR over LSF in patients afflicted by both hip and lumbar spine pathologies, as THR may ameliorate spinopelvic imbalances and reduce the risk of implant dislocation[39].

The possible role of the surgical approach to the hip

From the analysis of recent literature, it becomes evident that the surgical approach has not been extensively studied within the context of hip-spine relationships. The existing literature predominantly focuses on prosthetic replacement conducted through the postero-

lateral approach, with recommendations primarily aimed at preventing posterior dislocations. Conversely, the anterior, antero-lateral, and lateral approaches are less discussed and seemingly derive little benefit from current guidelines[40].
It is noted that there is a predominant focus on strategies for preventing posterior dislocation (anterior impingement) conceptualized for the postero-lateral approach[26].
Despite the presence of numerous registry studies aimed at assessing the survival of hip prosthetic implants in populations with altered hip-spine relationships, there have been few studies analyzing the influence of the surgical approach on this matter. The literature identifies two categories of patients: those termed "stuck standing" and those described as "stuck sitting." The former are characterized by the rigidity of the spinal-pelvic complex and therefore exhibit no alterations in pelvic tilt from the standing to the sitting position. The latter display abnormal pelvic tilt with negative values, indicating a retroverted posture during standing. Patients classified as "stuck standing" are found to be at higher risk for posterior dislocation[41]

How to place prosthetic components in patients with altered version and pelvic kinematics

The accurate categorization of patients based on their hip-spine type is crucial for the selection of the most appropriate implant positioning (Fig 1). Standard criteria for cup placement in THR typically involve a cup inclination of approximately 40° and anteversion of 20°. The "safe zone" for combined anteversion (calculated as the sum of the cup and stem sagittal anterior opening) is considered to fall within the range of 25° to 50°[42].
In accordance with the Phan classification system, a patient-specific algorithm for cup positioning is recommended based on overall sagittal balance and spinopelvic parameters[25]. In patients with normative sagittal alignment, the categories are as follows:
Type 1A: Patients with normal alignment and preserved spinopelvic mobility can be managed using conventional cup positioning of 20-25° of anteversion and an inclination of 40-45°. Type 1B: In cases with normal sagittal alignment but a rigid spine—where the change in sacral slope (SS) from standing to sitting is less than 10°—a more anteverted cup position is advised, approximately 30° of anteversion, to avert anterior impingement and subsequent posterior dislocation. Additionally, a cup inclination of 45° is recommended in the coronal plane. Group 2 pertains to patients with flatback deformity, characterized by a PI-LL greater than 10°: Type 2A: These patients with normal mobility should aim for 25-30° of anteversion from the functional pelvic plane (FPP), with a cup inclination of 40°.
Type 2B: For those with a rigid spine, greater anteversion is necessary to mitigate the risk of dislocation, with a recommended 30° of anteversion on the FPP and a 45° cup inclination. These patients are generally at a higher risk of dislocation, and the employment of specialized implants to minimize this risk is advised.
For comprehensive categorization, two additional types should be discussed[7,29]:
Hypermobility Type: Patients in this category exhibit a sacral slope change greater than 30° from standing to sitting. To prevent dislocation, a cup inclination of 35°-40° and anteversion of 15°-20° are recommended.
Anterior Pelvic Tilt Type: Typical in patients with hip flexion contracture, these individuals require cup positioning to align with the functional pelvic plane, targeting 20-25° of anteversion and a 40° inclination.

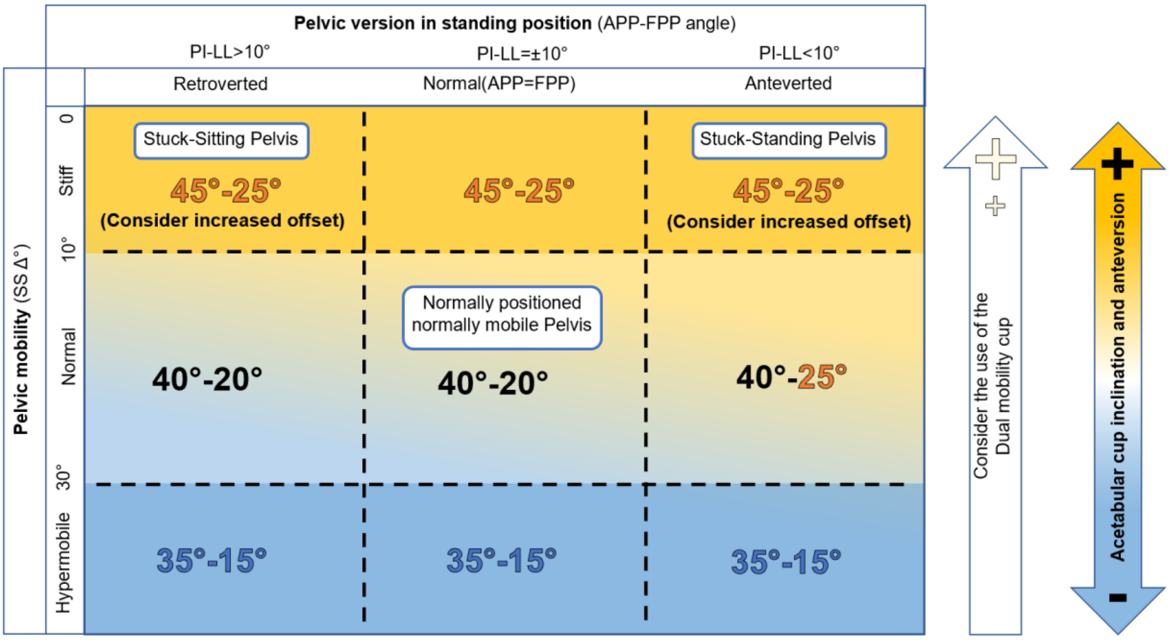

Fig1: Recommendations for performing total hip replacement: in each quadrant is indicated the recommended position for acetabular cup, namely inclination and anteversion, considering the APP. SS Δ°= angular difference in sacral slope between sitting and standing position, PI= Pelvic Incidence, LL= lumbar lordosis, APP= Anterior pelvic plane, FPP= Functional pelvic plane (in standing position).

The importance of a robust "in silico" experimental model

Despite the significance of clinical studies and expert recommendations, given the extreme complexity of the issue, the use of an "in silico" experimental model is becoming increasingly important. This has the potential to effectively simulate the relationship between the hip and spine, anticipating potential issues and providing valuable insights into the management of specific cases. It is evident that a one-size-fits-all approach is insufficient for ensuring accurate implant placement. Patient variability, encompassing both anatomical and functional aspects, necessitates a personalized approach. During surgical planning, considerations must include both the anticipated range of motion for the implant and the patient's expected post-operative mobility, as these factors significantly influence surgical outcomes. An implant, though mechanically sound, that restricts daily activities will not be well-perceived by the patient. Moreover, the actual range of motion for the implant cannot be tested intraoperatively.

To enhance surgical planning, advancements in computer modeling and simulation techniques have been made over the years[43]. Three-dimensional representations of relevant anatomical structures can assist clinicians during the pre-operative evaluation phase. Utilizing pre-operatively acquired medical images, such as CT scans, anatomically precise skeletal models can be generated. These models allow for quantitative assessments of the pre-operative and projected post-operative range of motion, factoring in the implant's planned positioning, patient-specific bony geometry, and the implant's design. Furthermore, computer simulations can identify joint configurations where contact between bone and implant, or bone-on-bone, occurs, thereby delineating the impingement-free zone. These digital twin models can simulate multiple scenarios, incorporating real-world motion data gathered from gait laboratories or wearable sensors.

Such simulations enable a more comprehensive understanding of anatomical and functional parameters influencing implant positioning.
While these simulation-based approaches show promise, their adoption in clinical settings remains limited due to the specialized skills needed to develop and implement these models. However, efforts are underway to streamline this process, and simpler workflows are expected to become available in the foreseeable future.
Concerning Finite Element (FE) models, several studies have explored their utility for understanding hip-spine relationships[44–47]. These computational models typically utilize patient-specific three-dimensional bone geometries and simplified musculoskeletal components. Applications range from biomechanical analysis of the spine, sacroiliac, and hip complex to risk assessments for hip joint diseases following spinal surgical interventions. For example, some studies have shown that variations in pelvic tilt can impact the mechanical stresses within the hip joint, particularly in cases of hip dysplasia. Others have used FE models to explore how spinal alignment affects biomechanical parameters at the hip joint.
Overall, while computational models offer valuable insights, further work is needed to simplify their application in a clinical setting. Advances in this area hold the promise of more personalized and effective surgical interventions, thereby enhancing patient outcomes.

EXPERIMENTAL STUDY

INTRODUCTION

This study arises from the need for a robust and representative experimental model of the general population for the precise investigation of the relationship between total hip replacement (THR) and pelvic version. The in-silico experimental models currently described in the literature do not sufficiently offer the robustness required to validate current clinical recommendations aimed at reducing the risk of impingement, instability, and dislocation in the surgical management of patients with pathological pelvic version or kinematics. Existing experimental models rely on three-dimensional reconstructions of the anatomy of individual patients or a cohort of patients, which are analyzed on a case-by-case basis, thereby hindering the generalizability of the results. The anatomy and biomechanics of the spinal-pelvic complex, the hip joint (and the lower limb in general), are highly variable, as evidenced by the wide variability in spinal-pelvic parameters and types of spinal alignment[48].
Another limitation of the experimental models currently described lies in the representation of the results and their potential clinical application. Indeed, the hip joint, being a ball-and-socket joint, presents highly complex biomechanics that are not easily conducive to an accurate understanding of possible movements in terms of range of motion. For instance, the commutative property is not applicable for all the geometric transformations of a sphere: if we rotate a sphere around one axis and then another, the order in which these rotations are executed influences the final outcome; therefore, rotations on a sphere are generally not commutative. Many studies have attempted to graphically represent the range of motion of a prosthetic joint, yet they often overlook the potential clinical value of the results.
With a robust and representative in-silico scientific model, it is possible to precisely and comprehensively assess the range of motion free of impingement of a hip prosthesis. Additionally, the selection of specific results allows for better interpretation of the data, in order to generate recommendations that are directly applicable in clinical practice, and that have the potential to either modify or confirm current medical practice.
Through this comprehensive approach, the study aims to make a meaningful contribution to the existing body of knowledge regarding the relationship between THR and pelvic version.

MATERIALS AND METHODS

We designed a tridimensional model in a free and open-source simulation environment. The simulation routine employed an array of specialized software and methodologies to ensure both the reliability and the reproducibility of our results. Each step was meticulously conducted, abiding by recognized standards, to ensure that the findings would not only hold scientific credibility but also offer clinically relevant insights. Different scenarios were simulated, and the range of motion of the prosthetic hip was assessed. In particular, we proceeded with the analysis of movements at particular risk of dislocation, and a study was conducted considering the range of motion of the femur allowed until contact (impingement) between geometries (discriminating bone-on-bone contact, implant-on-implant contact, and implant-on-bone contact). Furthermore, different pelvic version angles were evaluated to assess potential differences.

Geometry Retrieval for Simulation

The following three-dimensional geometries were employed for the conduction of this simulation framework: 3D models of hip prosthesis components (acetabular cup, liner, femoral head, and stem; representative and robust geometries of the pelvis and the femur of the adult population.

The authorization to use the CAD models of a prosthetic implant (Amistem, Mpact, Medacta International, Switzerland) was obtained. These components are widely used not only in Italy and Europe but also globally[49]. They represent the latest generation of prosthetic components and are often employed in minimally invasive approaches due to their reduced dimensions. The Mpact cup is a hemispherical press-fit acetabular cup made of a titanium alloy, coated with either hydroxyapatite or additive-manufactured 3D metal. The AMIStem is a straight, rectangular, cementless femoral stem, also made of a titanium alloy and coated with hydroxyapatite. The liner and femoral head are crafted from cutting-edge ceramic materials (Delta series) and are manufactured by CeramTec[50]. The liner is accommodated within the acetabular cup, while the femoral head has a specific interlocking mechanism with the stem's neck, known as the trunnion.

The bone model was extracted using Map Client software. The MAP Client is the client-side application of the musculoskeletal atlas project(MAP)[51]. It is a versatile cross-platform framework for managing workflows, written in Python and leveraging the robust capabilities of Qt, the MAP Client offers a plugin-based architecture. This framework enables the construction of workflows through an integration of workflow steps, each serving as a modular plugin within the system. These plugins can execute a diverse range of tasks, from simple data manipulations to intricate computational processes, offering the user a scalable tool adaptable to different scientific inquiries. Other features of the MAP Client is its focus on user-generated content. The application is designed to facilitate the easy development and integration of custom plugins into the workflow. By keeping the prerequisites for creating workflow steps as minimal as possible, the platform allows developers to concentrate on the practical aspects of their tasks. To expedite this process, the MAP Client includes a Plugin Wizard tool, which automates the generation of the foundational code structure required for a new workflow step. This emphasis on a plugin-based architecture also encourages collaborative research. It allows research groups to effortlessly share both complete workflows and individual workflow steps, thereby fostering an environment of open science and inter-disciplinary cooperation. Moreover, the

decentralization of plugin development serves to reduce reliance on an external development team, enabling the scientific community to directly contribute to the tool’s evolution.
The bone model utilized (pelvis and femur) was generated using MAP Client (statistical average model of adult bones from 200 CT scans), which enabled the creation of highly representative and robust geometries of the adult population. This model was incorporated into the simulation environment, and the prosthetic components were positioned according to the appropriate surgical planning.
The model employed has specific dimensions as it is extracted from a pool of CT scans, which are tests with intrinsic and reliable image magnification. The extracted model presents the following spinopelvic parameters, considering the anterior pelvic plane parallel to the vertical: Pelvic Incidence (PI) 53.5°°; Sacral Slope (SS) 40°; Pelvic Tilt (PT) 13.5°. The only femoral parameter measured was the anteversion of the femoral neck relative to the condylar plane, which was found to be 13.2°.
It should also be specified that the model used has modifiable characteristics, automatically generated by the MAP client based on the statistical analysis of the 200 CT scans. These adjustable parameters allow for the recreation of all the analyzed bone segments and also possible intermediate geometries, according to a Gaussian statistical distribution, which is characteristic of most biological parameters. Specifically, dimensions and proportions can be altered, and the model can also be oriented in space along the three planes, thereby generating different spinopelvic parameters. These models can be easily utilized for simulations by employing the same routine described in the subsequent parameters. It is also conceivable to conduct a study of populations by generating an "in-silico trial."

Simulation Routine

The simulation process employed a set of specialized software packages in a sequential manner to accomplish various tasks. The following outlines the routine in a stepwise manner.

Component Positioning and Virtual Planning

For initial positioning and virtual planning of prosthesis components within the bone model, Materialise's Mimics 24 and Mimics Innovation Suite (MIS) were utilized (Mimics 24, mimics innovation suite MIS, Materialise NV, Leuven, Belgium)[52]. The Mimics Innovation Suite (MIS) offers an integrated, end-to-end workflow that incorporates image-based design and 3D printing capabilities. The suite includes additional software modules that can interface with Mimics 24 for further analysis, including biomechanical simulations. All analyses were performed in accordance with the guidelines and protocols provided by the software developer, ensuring reproducibility and standardization of the outcomes." These software packages allow for high-precision alignment, positioning, and orientation of prosthesis components, thereby ensuring accurate representation within the simulation environment. Also, it is specifically designed for processing and editing medical imaging data, allowing for the conversion of Digital Imaging and Communications in Medicine (DICOM) files into high-fidelity 3D models. The software provides advanced segmentation algorithms and tools for accurate region-of-interest extraction. It also enables the application of various filters and thresholding techniques to isolate and delineate complex anatomical features. The software allows for 3D models optimization by manual editing to

ensure the anatomical accuracy. The generated 3D models were exported in the Standard Tessellation Language (STL) format for further biomechanical analysis.
The prosthetic components were positioned according to an appropriate surgical plan conducted by a surgeon experienced in three-dimensional planning[20]. Starting from the bone geometries, the center of rotation of the joint was determined, and based on this, the prosthetic joint was reconstructed. The acetabular component was selected from various sizes, taking into account the appropriate removal of the superficial acetabular bone tissue and proper orientation relative to the acetabular rim, so as to respect its anatomy. On the acetabular component, the liner was positioned in accordance with the complementary geometry of the components, maintaining coplanarity on the equatorial plane and concentricity with the native joint's center of rotation. The stem was positioned after a virtual osteotomy of the femoral neck, with an inclination of 45 degrees relative to the diaphyseal axis, and oriented in anteversion equal to that of the native neck. In the cranio-caudal direction, 1 cm of the neck was maintained from the proximal base of the lesser trochanter. The size of the stem and its orientation on the three planes were selected based on its ability to fill the diaphyseal canal, while maintaining adequate anteversion, and sinking the component to respect the line of virtual osteotomy and allow the concentricity of the native joint's center of rotation using an M-head (0 offset).
The prosthetic components were not resized but were selected based on the dimensions of the bone geometries, allowing choices from various sizes present in the Medacta database. The components used were Mpact two holes with a diameter of 50mm, Amistem-C size 5 standard (non-lateralizing), ceramic M-head (0 offset) 32 mm, and ceramic liner 32 mm (Fig 2) (Fig 3).
The choice of a 32 mm articulation, as opposed to the option of using a 36 mm joint interface (which offers better range of motion and stability characteristics), was dictated by the need to highlight any potential conflicts (impingement) more effectively between prosthetic components, particularly between the stem collar and the acetabular component liner. This decision to utilize a less favourable joint interface is supported by additional studies and allows for more robust results.[53]

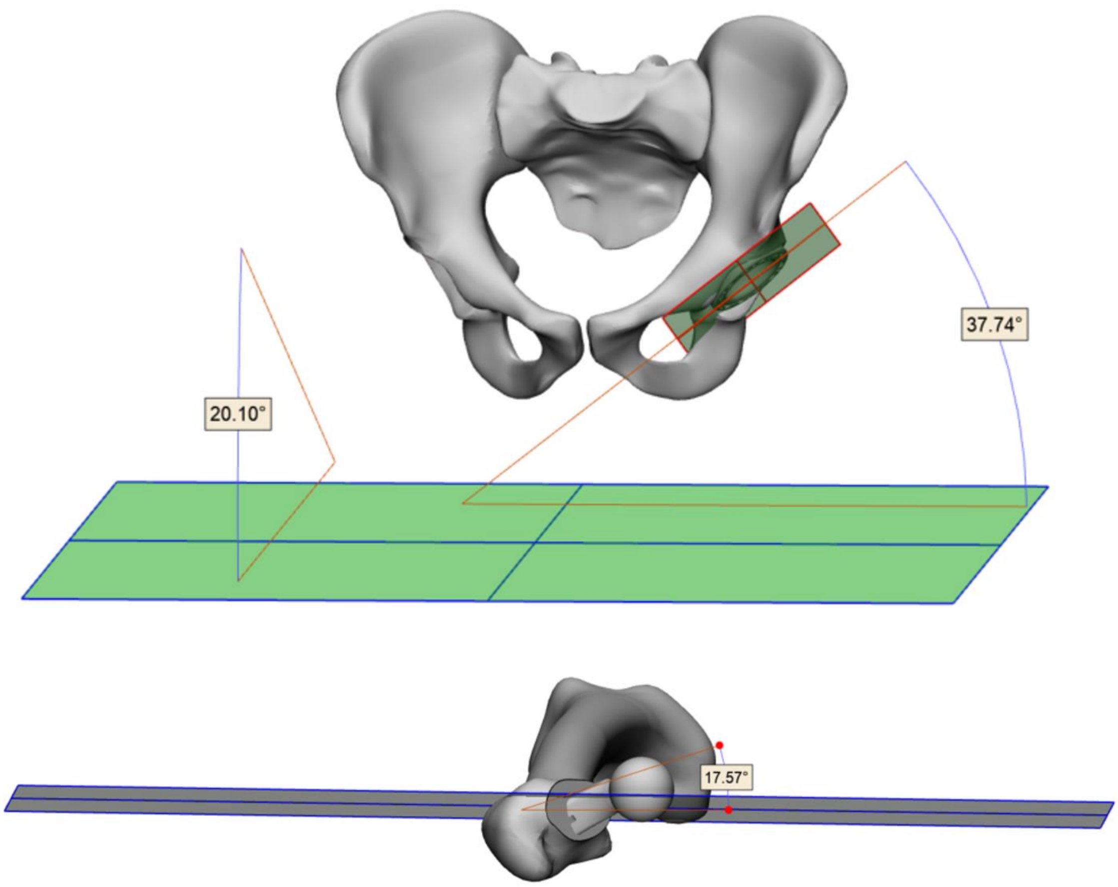

Fig 2: The orientation of the pelvis in space was maintained with the anterior pelvic plane parallel to the vertical axis of the reference system. In this manner, by utilizing the function for projecting geometries onto the frontal and sagittal planes, the final position of the components was found to be 37.74 degrees of inclination and 20.10 degrees of anteversion for the acetabular component, and 17.57 degrees of anteversion for the femoral component.

Component Merging

Following the virtual planning stage, the individual components were merged together using 3-matic V17, also part of Materialise's Mimics Innovation Suite. This merging process ensures that the components are coherently and appropriately aligned to produce an accurate and unified 3D model for simulation.

3-matic V17[54] is an advanced software tool specifically designed to facilitate the manipulation, design optimization, and analysis of 3D models. It allows for a range of capabilities including smoothing, remeshing, and the application of parametric design modifications, among other features. In this study, 3-matic V17 was employed to refine the anatomical structures, improve mesh quality, and perform finite element analyses (FEA). Surface smoothing algorithms were applied to reduce noise and improve the fidelity of the reconstructed anatomical features. Boolean operations were executed for merging or subtracting different geometrical entities as needed for the biomechanical analysis. The software was also used to generate high-quality meshes with tetrahedral and hexahedral elements, optimizing the model for subsequent finite element biomechanical simulations, which, however, are not the objective of the present study.

Surface Mesh Optimization and Compatibility

The software MeshLab was employed to fine-tune the mesh surfaces of the combined 3D models. This software was critical for optimizing mesh properties, ensuring compatibility between different components, and enhancing computational efficiency.

MeshLab[55] software is an open-source mesh processing system developed by the Visual Computing Lab - ISTI-CNR. MeshLab is employed for a variety of mesh editing tasks, such as cleaning, smoothing, and remeshing, to optimize the 3D models for subsequent analyses. Specifically, the software was utilized to remove isolated mesh components, fill gaps, and correct topological errors, thereby enhancing the quality and integrity of the mesh structures. The software also provides advanced algorithms for mesh simplification, surface reconstruction, and geometric transformations, which were selectively applied based on the specific requirements of the study.

MeshLab was used for conducting preliminary analyses to evaluate mesh quality metrics, including the distribution of vertices and the regularity of facets, which were critical for ensuring that the models met the criteria for the biomechanical simulations. The software's built-in scripting capabilities were harnessed to automate repetitive tasks and ensure standardization and reproducibility across multiple models. All procedures were performed according to the protocols and guidelines suggested by the MeshLab development team to guarantee the accuracy and reliability of the results.

Biomechanical Model Adaptation

A Matlab Application Programming Interface (API), utilizing the Staple Toolbox along with methodologies from Modenese and Renault[56], was applied for biomechanical adaptation of the hip model. This computational tool designed to automate the generation of patient-specific musculoskeletal models of the lower limb ensures that the model reliably reflects the actual biomechanical conditions of the human hip.

The traditional methods for creating these models are often labor-intensive and require a significant amount of time and expertise, limiting their widespread adoption. This tool streamlines these processes by directly translating three-dimensional bone geometries, typically obtained from segmented medical images, into fully functional musculoskeletal models. The tool's efficacy was assessed by comparing its outputs with four manually constructed lower limb models[56].

The tool is implemented in the MATLAB scripting language and executes within seconds, eliminating the need for operator intervention. It produces lower extremity models that are immediately suitable for kinematic and kinetic analysis, as well as for serving as baselines for more advanced musculoskeletal modelling approaches.

Contact Model and Simulation Volume Definition: Matlab and OpenSim v4.3 were employed to define the contact model and the volumes considered for simulation. The Delp[57] and Seth[58] guidelines were followed for these aspects, creating a comprehensive and valid framework for the simulation.

MATLAB is a high-level numerical computing environment and programming language developed by MathWorks, Inc. MATLAB was employed for its extensive array of built-in functions and toolboxes specifically designed for scientific and engineering computations. The platform offers an integrated development environment (IDE) with a rich set of tools for data visualization, analysis, and algorithm development. Custom scripts and functions were created within MATLAB to preprocess the data, perform statistical analyses, and execute complex simulations.

OpenSim[59] is an open-source software platform developed by the National Center for Simulation in Rehabilitation Research at Stanford University. OpenSim provides a robust framework for the development, analysis, and simulation of complex musculoskeletal models. The software is specifically tailored to facilitate the investigation of the neuromuscular control, kinematics, and biomechanics of various movement tasks. Pre-existing musculoskeletal models provided within the OpenSim software package were utilized as the foundational basis for our study, and where necessary, were modified to match the specific anatomical and biomechanical parameters of our simulation model. All custom scripts, parameter files, and simulation setups were implemented within the OpenSim graphical user interface and scripting API. OpenSim serves also as a foundational framework that enables the biomechanical research community to develop, share, scrutinize, and refine a comprehensive repository of simulations via collaborative efforts across multiple institutions.

For the purposes of this study, the following regions of interest were defined among the various geometries: bone-on-bone (pelvis versus femur); implant-on-implant (equatorial edge of the acetabular component and acetabular liner against the neck of the prosthetic stem); and implant-on-bone (neck of the prosthetic stem against the pelvis, equatorial edge of the acetabular component and acetabular liner against the femur) (Fig. 3).

Fig 3: The geometries were parameterized in order to define the contact, distinguishing bone-on-bone, implant-on-implant and implant-on-bone impingement.

Simulation Parameterization

OpenSim v4.3, corroborated by the guidelines from Delp[57] and Seth[58], was instrumental in defining the specific parameters for simulation, such as load distribution, motion constraints, and kinematics.
The following movements were analysed: Pure flexion (till 120°), Flexion in 5° abduction and 15° internal rotation (rising from a sitting position), Flexion in 10° adduction and 25° internal rotation (Stooping), Flexion in 15° adduction and 15° internal rotation (tying shoes), Flexion in 15° adduction and 15° external rotation (crossing legs), Internal rotation (Till120°) in 90° of flexion and neutral abduction, Pure extension (till 90°), External rotation in 15° extension and 5° abduction(pivoting in a standing position), External rotation in 5° extension and 5° adduction (rolling over in bed).
In accordance with biomechanical society guidelines, movements are represented by both positive and negative values relative to the starting anatomical position. Specifically, for the flexion-extension movement, negative values denote extension while positive values represent flexion (+F/-E). Similarly, for adduction-abduction, positive values signify adduction and negative values indicate abduction (+AD/-AB). In the case of rotations, positive values are allocated to external rotation and negative values to internal rotation (+ER/-IR). This standardized nomenclature is essential for the accurate interpretation and comparison of biomechanical data in orthopedic studies.
These are movements associated with dislocation, well-described in the literature by Nadzadi et al. [60], also employed in the methodology of various studies[61,62].The movements in question have significant clinical relevance and enable straightforward interpretation of the data. This methodology was chosen for two primary reasons: first, simulating all possible movements would require substantial computational resources; and second, the results obtained from a complete analysis of all possible movement combinations would be difficult to interpret and have little clinical significance. Thus, focusing on these specific movements, on a single plane, allows for a more targeted and meaningful analysis in line with the objectives of the study.
These movements have been categorized into two groups based on their potential to produce either posterior or anterior dislocation. Specifically, the following movements may lead to posterior dislocation: Pure flexion (till 120°), Flexion in 5° abduction and 15° internal rotation, Flexion in 10° adduction and 25° internal rotation, Flexion in 15° adduction and 15° internal rotation, Flexion in 15° adduction and 15° external rotation, Internal rotation (Till120°) in 90° of flexion and neutral abduction. On the contrary, these others are likely to result in anterior dislocation: Pure extension (till 90°), External rotation in 15° extension and 5° abduction, External rotation in 5° extension and 5° adduction.
These movements were analyzed in three distinct pelvic configurations: Neutral pelvis with the Anterior Pelvic Plane (APP) parallel to the vertical axis, featuring pelvic incidence (PI) of 53.5°°, sacral slope (SS) of 40°, and pelvic tilt (PT) of 13.5°; Anteverted pelvis with the APP tilted +10° relative to the vertical axis, and with PI of 53.5°°, SS of 50°, and PT of 3.5°; Retroverted pelvis with the APP tilted -10° relative to the vertical axis, and with PI of 53.5°°, SS of 30°, and PT of 23.5° (Fig 4). Each of these configurations was meticulously examined to provide a comprehensive understanding of how different pelvic orientations could impact the movements under study.

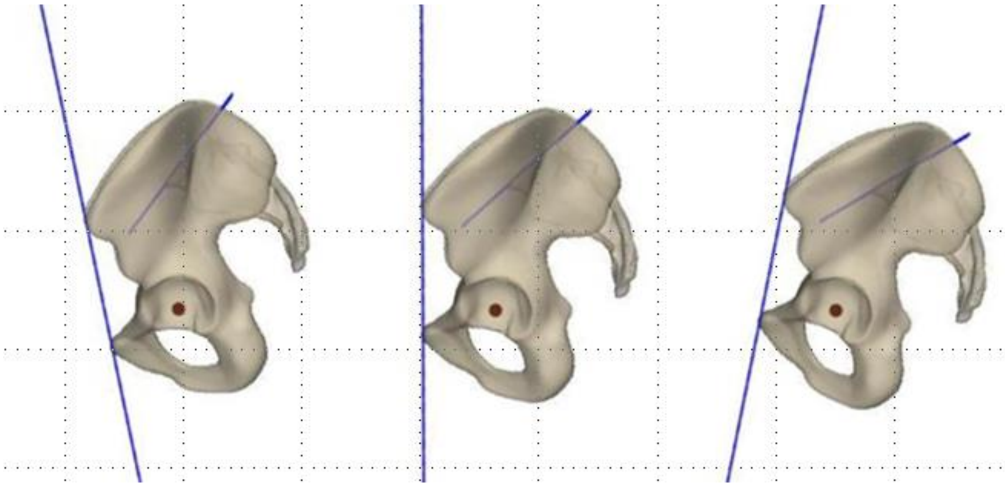

Fig 4: The ranges of motion up to contact, for the different movements prone to dislocation, were evaluated considering three different pelvic configurations, in anteversion (+10°), neutral and retroversion (-10°), in the image represented from left to right.

Simulation Execution

Simulations were conducted using OpenSim v4.3 software. The simulation scenarios were initiated, examining each type of studied movement for three different categories of impingement: bone-on-bone, implant-on-implant, and implant-on-bone.

Movements were constrained by considering extreme range of motion, to force impingement. Specifically, the limitations imposed were: 120° for flexion, 65° for extension, 60° for external rotation, and 60° for internal rotation

Data regarding the forces generated at the various study interfaces (contact models) were extracted and subjected to preliminary analysis. Real-time monitoring of the simulation scenario was conducted to assess the reliability of the results. Upon initial analysis, we encountered a significant issue concerning the articular interface between the prosthetic head and the insert. Although these components were concentric (with a virtual space at their interface), they generated contact forces between the geometries that complicated data interpretation. This issue presents a challenging obstacle, one that has also been noted by other authors in previous studies. The complex nature of these forces warrants further scrutiny to refine the computational models and offer clinically relevant insights[61].

Herein, we investigated two specific approaches to resolving articular interface problems: a 32mm femoral head on a 36mm liner while maintaining the same rotation center, or the removal of the femoral head from contact recording altogether.

Given the significance of the 32mm liner within the context of the study, the decision was made to proceed with the removal of the prosthetic head while maintaining the same center of rotation and associated mechanical constraints. The outcomes of the updated simulated scenarios enabled the generation of effective results that are aligned with the study's objectives. This modification served to eliminate the confounding variables introduced by the prosthetic head, thereby enhancing the validity and interpretability of the generated data.

Data Extraction and Filtration

Post-simulation, data was extracted in *.STO format using OpenSim v4.3 software.

The STO file format was employed for the storage and management of time-series data throughout the study. This ASCII-based text file format, commonly used within the

OpenSim biomechanical modeling and simulation framework, allows for the tabular representation of temporal data, including but not limited to muscle forces, joint angles, and kinematic variables. Each STO file consists of metadata headers that provide essential information regarding the columns and units of the data set, followed by the time-step indexed data entries. This format offers ease of integration with various data analysis tools and scripting languages, including MATLAB and Python, enabling efficient data extraction and computational analysis.
Microsoft Excel was then employed to filter these data, isolating key metrics for further analysis.

Data Analysis
Microsoft Excel was extensively used for further data manipulation and preparation. This involved generating descriptive statistics, distributions, and preliminary interpretations to present an overarching view of the results.

Data Interpretation
The final interpretation of the data was performed using both Excel. These platforms enabled a range of statistical analyses to be performed, providing depth to our study and robustness to our findings.

Summary of methods
In summary, our simulation routine employed an array of specialized software and methodologies to ensure both the reliability and the reproducibility of our results. Each step was meticulously conducted, abiding by recognized standards, to ensure that the findings would not only hold scientific credibility but also offer clinically relevant insights. Through this comprehensive approach, the study aims to make a meaningful contribution to the existing body of knowledge regarding hip prostheses and their implications for patient mobility and potential risk of impingement and dislocation.

RESULTS

The results of the various simulation scenarios are presented in Tables 1,2 and 3.
Each table displays data for the movements under study for a specific pelvic position (Neutral pelvis, Anteverted pelvis, Retroverted pelvis). In each of the three columns, angular values at which impingement occurs are identified. It should be noted that for each specific movement being studied, there is a single plane of movement while the other two axes of movement remain fixed. A color-coding scheme is employed to visually distinguish between movements that are Free of Impingement (FOI) (highlighted in green) and those where impingement occurs (highlighted in orange). Additionally, the angle at which impingement occurs most prematurely among the three types of impingements studied is emphasized in red, so to highlight their clinical significance.
In Table 4, the angles and types of impingements that first occur for each dislocating movement are highlighted across the three pelvic version configurations.
In Table 5, the sum of the absolute value of the angle at which contact occurs most prematurely for each pelvic configuration is presented, distinguishing between movements predisposing to posterior or anterior dislocation.
In total, 81 simulations were performed, represented by the combination of the nine dislocated movements with the three different types of impingement and three pelvic versions.

The anteverted pelvis demonstrated at least one contact between geometries in 6 out of 9 (66.7%) movements, the retroverted pelvis in four (44.4%), while the neutral pelvis in three (33.3%).
The anteverted pelvis also exhibits smaller range of motion considering the sum of the absolute values of the angles at which any type of impingement firstly occurred (Table 4), thus indicating a greater overall risk. Considering only movements predisposing to anterior dislocation the retroverted pelvis displays reduced angles, conversely, movements linked to posterior dislocation demonstrate smaller angles in the anteverted pelvis.
Considering all movements and the different types of impingements, it was observed that the retroverted pelvis exhibited the highest incidence of impingements, accounting for 10 out of 27 cases (37%), the anteverted pelvis showed impingements in 9 out of 27 cases (33%), whereas the neutral pelvic position demonstrated the lowest occurrence of contact between geometries, with 6 out of 27 cases (22.2%).

In 6 out of 13 cases (46.1%), implant-on-bone contact was the initial impingement type observed within the studied range of motion for each specific movement. Conversely, bone-on-bone impingement occurred first in 5 cases (38.5%). Implant-on-implant impingement, which occurs at wider angles or is absent altogether, was relevant in only 2 simulations (15.4%).
Flexion movements result in implant on bone contact between geometries only in the case of anteverted pelvis. Internal rotation movement involves contact between geometries in all three pelvic configurations, with earlier bone-on-bone contact and smaller angles occurring in the retroverted pelvis. Pure extension is the only movement to induce early contact between implant and implant, with smaller angles observed in the retroverted pelvis.
External rotation movements show primary implant-on-bone contact in the retroverted pelvis, while demonstrating early bone-on-bone contact in the neutral and anteverted pelvis.

	APP:0 Pelvic Tilt 13.5°								
	Implant-on-implant			implant on bone			Bone-on-bone		
kinematic activity associated with dislocation	Adduction	Rotation	Flexion	Adduction	Rotation	Flexion	Adduction	Rotation	Flexion
a Pure flexion (till 120°)	0	0	FOI	0	0	FOI	0	0	FOI
b Flexion (till 120°) in 5° abduction and 15° internal rotation	-5	-15	FOI	-5	-15	FOI	-5	-15	FOI
c Flexion (till 120°) in 10° adduction and 25° internal rotation	10	-25	FOI	10	-25	FOI	10	-25	FOI
d Flexion (till 120°) in 15° adduction and 15° internal rotation	15	-15	FOI	15	-15	FOI	15	-15	FOI
e Flexion (till 120°) in 15° adduction and 15° external rotation	15	15	FOI	15	15	FOI	15	15	FOI
f Internal rotation (Till 60°) in 90° of flexion and neutral abduction	0	-57	90	0	FOI	90	0	-55	90
g Pure extension (till 65°)	0	0	-64	0	0	FOI	0	0	FOI
h External rotation (till 60°) in 15° extension and 5° abduction	-5	49	-15	-5	42	-15	-5	34	-15
i External rotation (till 60°) in 5° extension and 5° adduction	5	FOI	-5	5	FOI	-5	5	FOI	-5

Table 1: Angles and Types of Impingement in Various Study Movements with the Pelvis in a Neutral Position

	APP: -10 retroverted Pelvic Tilt 23.5°								
	Implant-on-implant			implant on bone			Bone-on-bone		
kinematic activity associated with dislocation	Adduction	Rotation	Flexion	Adduction	Rotation	Flexion	Adduction	Rotation	Flexion
a Pure flexion (till 120°)	0	0	FOI	0	0	FOI	0	0	FOI
b Flexion (till 120°) in 5° abduction and 15° internal rotation	-5	-15	FOI	-5	-15	FOI	-5	-15	FOI
c Flexion (till 120°) in 10° adduction and 25° internal rotation	10	-25	FOI	10	-25	FOI	10	-25	FOI
d Flexion (till 120°) in 15° adduction and 15° internal rotation	15	-15	FOI	15	-15	FOI	15	-15	FOI
e Flexion (till 120°) in 15° adduction and 15° external rotation	15	15	FOI	15	15	FOI	15	15	FOI
f Internal rotation (Till 60°) in 90° of flexion and neutral abduction	0	-56	90	0	-60	90	0	-53	90
g Pure extension (till 65°)	0	0	-55	0	0	-62	0	0	FOI
h External rotation (till 60°) in 15° extension and 5° abduction	-5	49	-15	-5	34	-15	-5	39	-15
i External rotation (till 60°) in 5° extension and 5° adduction	5	FOI	-5	5	53	-5	5	58	-5

Table 2: Angles and Types of Impingement in Various Study Movements with the Pelvis in a retroverted Position

	APP: +10 anteverted Pelvic Tilt 3.5°								
	Implant-on-implant			implant on bone			Bone-on-bone		
kinematic activity associated with dislocation	Adduction	Rotation	Flexion	Adduction	Rotation	Flexion	Adduction	Rotation	Flexion
a Pure flexion (till 120°)	0	0	FOI	0	0	FOI	0	0	FOI
b Flexion (till 120°) in 5° abduction and 15° internal rotation	-5	-15	FOI	-5	-15	118	-5	-15	FOI
c Flexion (till 120°) in 10° adduction and 25° internal rotation	10	-25	FOI	10	-25	113	10	-25	FOI
d Flexion (till 120°) in 15° adduction and 15° internal rotation	15	-15	FOI	15	-15	112	15	-15	FOI
e Flexion (till 120°) in 15° adduction and 15° external rotation	15	15	FOI	15	15	117	15	15	FOI
f Internal rotation (Till 60°) in 90° of flexion and neutral abduction	0	-56	90	0	FOI	90	0	-54	90
g Pure extension (till 65°)	0	0	FOI	0	0	FOI	0	0	FOI
h External rotation (till 60°) in 15° extension and 5° abduction	-5	51	-15	-5	49	-15	-5	32	-15
i External rotation (till 60°) in 5° extension and 5° adduction	5	FOI	-5	5	FOI	-5	5	FOI	-5

Table 3: Angles and Types of Impingement in Various Study Movements with the Pelvis in a anteverted Position.

	first type of impingement that occurs		
kinematic activity associated with dislocation	neutral	retroverted	anteverted
a Pure flexion (till 120°)	FOI	FOI	FOI
b Flexion (till 120°) in 5° abduction and 15° internal rotation	FOI	FOI	IOB 118
c Flexion (till 120°) in 10° adduction and 25° internal rotation	FOI	FOI	IOB 113
d Flexion (till 120°) in 15° adduction and 15° internal rotation	FOI	FOI	IOB 112
e Flexion (till 120°) in 15° adduction and 15° external rotation	FOI	FOI	IOB 117
f Internal rotation (Till 70°) in 90° of flexion and neutral abduction	BOB -55	BOB -53	BOB -54
g Pure extension (till 65°)	IOI -65	IOI -55	FOI
h External rotation (till 60°) in 15° extension and 5° abduction	BOB 34	IOB 34	BOB 32
i External rotation (till 60°) in 5° extension and 5° adduction	FOI	IOB 53	FOI

Table 4: Angles and types of impingement occurring for each dislocating movement considering the three pelvic version configurations. Movements that are free from impingement (FOI) are highlighted in green, those where impingement occurs are highlighted in orange, while for each movement, the angle at which impingement occurs most prematurely among the three types of pelvic version is emphasized in red. The type of impingement precedes the angular values: IOB: Implant-on-Bone, BOB: Bone-on-Bone, IOI: Implant-on-Implant.

	Total	**Posterior dislocation prone movements**	**Anterior dislocation prone movements**
Neutral pelvis	813	655	158
Retroverted pelvis	795	653	**142**
Anteverted pelvis	**791**	**634**	157

Table 5: The sum of the absolute value of the angle at which impingement occurs most prematurely for each pelvic configuration is presented, distinguishing between movements predisposing to posterior or anterior dislocation. In the case of movements free of impingement (FOI), the constrained angle for that specific movement was considered. The smaller the sum of the angles, the smaller the articular range leading up to impingement. For each column, angles that are smaller are highlighted in bold.

DISCUSSION

The present study provides a precise and reproducible experimental model characterized by high robustness and representativeness. The preliminary results presented allow for an appreciation of the validity of the simulation environment and the clear and effective mode of data presentation.
In the analysis of the results from the three pelvic orientation configurations, the importance of the sagittal orientation of the pelvis in maintaining the joint stability of the prosthetic joint has been highlighted.
In the analysis of the results, it was found that 6 out of the 9 movements studied produced (any type of) impingement in the anteverted pelvis, whereas the retroverted pelvis showed impingement in 4 movements, and the neutral pelvis in 3 movements. The anteverted pelvis also showed the smaller overall range of motion until impingement, in particular concerning movement prone to anterior dislocation, while the retroverted pelvis displays smaller angles in movements associated with anterior dislocation. The pelvic orientation with the fewest contacts between geometries and higher range of motion in different simulation scenarios was the neutral pelvis.
Considering all the possible impingement type (BOB, IOB, IOI) in the different simulation scenarios, the retroverted pelvis was found to be the one with the highest number of contacts.
In most instances within the examined range of motion for each individual movement, the initial (and clinically relevant) type of impingement encountered was the implant-on-bone type. Conversely, implant-on-implant impingement occurs at more extreme angles, or do not occur at all, although it represents the primary point of contact between the geometries during pure extension movement.

Limitation of the study

The limitations of the present study are numerous and should be clearly understood for accurate interpretation of the results. The experimental geometric model adopted is singular (although it exists in three different sagittal orientations) and is based on the statistical average of 200 CT scans performed with the subject in the supine position. The geometries presented may not reflect the characteristics of any actual human being, as the experimental model is not a digital twin, nor has an 'in-silico trial' been conducted. Additionally, there is no information regarding the spatial orientation of the bone segments, which have been defined based on the assumption that the anterior pelvic plane is parallel to the vertical axis and that the condylar plane of the femur is parallel to the frontal plane of the reference system.
Another limitation is that this is not a finite element analysis but simply a contact analysis between geometries. Finite element analysis has the potential to generate more reliable results concerning the possible outcomes following contact between geometries, more precisely defining the potential progression of impingement toward conditions of simple instability/subluxation or toward actual dislocation of the implant. Indeed, instability or dislocation are multifactorial complications where mechanical contact between bone and prosthetic elements represents only one of the possible causes for temporary or complete loss of articular relationships. Moreover, the contribution of soft tissues (capsule, muscles,

and tendons) in terms of possible resistance to dislocating movements or as a cause of mechanical conflict is not assessed.
Further limitations of the study stem from the monoplanar analysis of a limited set of movements that are potentially dislocating. This simplification has, however, allowed for the extraction of clinically significant data while avoiding potentially confusing and difficult-to-interpret information. Additionally, a single placement of the prosthetic components has been evaluated, and simplifications were made to the model by removing the prosthetic head to enhance the efficiency of the simulation.
While the study may seem overly simplified, it is a critical optimization of the experimental model aimed at eliminating potential confounding parameters, thereby giving greater emphasis to findings that have clinical relevance.

Bone geometry
The bone model used, although comprising only the pelvis and femur, appears to be representative of the anatomy and biomechanics of the study region. In particular, the spinopelvic parameters appear to be within the average range, considering a pelvic incidence (PI) of 53.5°, a sacral slope (SS) of 40°, and a pelvic tilt (PT) of 13.5°. It should be noted that the orientation of the pelvis in space is based on the assumption that the anterior pelvic plane is parallel to the vertical axis. The sagittal orientation is not derived from CT scans using the Map client software, which utilizes images acquired with the patient in the supine position. Additionally, the pelvic incidence, the sole anatomical angular parameter, is in agreement with what is described in the literature[63].
Concerning the femur, the observed anteversion value of 13.5° relative to the condylar plane falls within the average anatomical range. The strength of the geometric model extracted from the MAP client lies in its ability to define an average bone geometry with adjustable attributes, which are auto-generated by the MAP client through statistical analysis of 200 CT scans. These tunable parameters enable the reconstitution of all examined bone segments, as well as potential intermediary geometries, in accordance with a Gaussian statistical distribution commonly seen in biological parameters. Specifically, alterations can be made to dimensions and proportions, and the model can be spatially oriented along all three planes, thereby yielding varying spinopelvic parameters. Such models are readily amenable to simulation exercises using the same methodology delineated in subsequent parameters. Moreover, it is feasible to conduct population-based studies by creating an "in-silico trial."

Pelvic orientation on the risk of impingement
In the analysis of the results from the three pelvic orientation configurations, the importance of the sagittal orientation of the pelvis in maintaining the joint stability of the prosthetic joint has been highlighted.
The anteverted pelvis exhibited contact between geometries in 6 out of 9 studied movements (66.7%), the retroverted pelvis in four movements (44.4%), while the neutral pelvis in three movements (33.3%). Also, the position of the pelvis in anteversion presented reduced overall range of motion until contact, in particular in relation to posterior dislocating movements. On the contrary, the retroverted pelvis displays reduced range of motion until impingement considering posterior dislocating movements.

The presented data also confirms that a normally aligned pelvis, with pelvic tilt within normal limits and a vertical APP, represents as a protective factor against adverse events such as impingement, instability, and dislocation[40]. At the same time, it seems appropriate to hypothesize that the anteverted pelvis represents the pelvic version with the greatest risk, although the retroverted pelvis exhibited the highest number of impingements in the different simulation scenarios.

There is a lack of studies in the literature with similar methodologies that would allow for a direct comparison of results. The studies that do exist employ non-standardized methodologies, which hinder the effective aggregation of knowledge.
In the study conducted by Pryce et al.[61], the range of motion until impingement is demonstrated across diverse configurations of acetabular inclination and anteversion, additionally spotlighting the contact point in relation to various movements. A noteworthy limitation of the study in question is its reliance on data from a single geometric model, randomly sourced from a data repository, and the analysis of only implant to implant impingement. This limitation underscores the need for more standardized research approaches in this field to facilitate more reliable comparisons and contribute to a more comprehensive understanding of the problem.

Type of impingement

In most cases, the first type of impingement that occurs in the studied range of motion was implant-on-bone impingement, while implant-on-implant impingement occurred at greater angles or did not occur at all.
The simulation study highlighted some patterns considering that various movements result in different types of impingement depending on the pelvic configuration.

Implant-on-implant impingement resulted clinically significant only in pure extension movement in the neutral and retroverted pelvis, in which it represents the primary contact between geometries.
This type of impingement consisted in the mechanical conflict between the femoral neck and the postero-inferior margin of the acetabular component, being exclusively dependent on the mutual orientation (combined anteversion) of the components (not being influenced by bone morphology) and can lead to anterior dislocation. In consideration of this, special attention must be paid to this type of impingement when performing surgical approaches predisposing to anterior dislocation (anterior, lateral and antero-lateral approach), considering also that it may be beneficial to reduce anteversion and inclination of the acetabular component[61].

Implant-on-bone was the only type of impingement that resulted clinically significant in flexion movement in the anteverted pelvis, while in external rotation movements it resulted clinically significant in the retroverted pelvic scenarios.
This type of impingement consisted of the contact between the prosthetic neck and the anterior wall of the acetabulum in flexion movements, while the posterior wall was involved in external rotation movements, so that this kind of impingement can be responsible for both posterior and anterior dislocation.

In consideration of this, the importance of adequate removal of acetabular osteophytes is confirmed, both in patients with anteverted rigid pelvis (stuck sitting) predisposed to posterior dislocation (posterolateral approach), and in patients with rigid retroverted pelvis (stuck standing), as well as paying particular attention to the appropriate version of the femoral component.

Bone-on-bone impingement resulted clinically significant in internal rotation movement across all pelvic configurations, while in external rotation movements, it resulted clinically significant in anteverted and neutral pelvic scenarios.
In patients at risk for BOB impingement, it is advisable to perform dynamic stability tests, assessing rotations movements associated with various degrees of flexion-extension and adduction-abduction. To reduce the risk of BOB impingement, a possible solution involves increasing the distance between the greater trochanter and the pelvis (particularly the ischium), modifying not so much the orientation but rather the offset of the prosthetic joint.

It is also interesting to note how the type of clinically significant impingement varies in relation to pelvic configuration: for example, in movements involving external rotation, it is possible to observe a progression from implant-on-bone impingement to bone-on-bone impingement, transitioning from a retroverted pelvic configuration to an anteverted one.

These results can be compared to recent studies [62, 64] that analyzes the types of impingement after THR. However, these studies do not examine implant-on-bone impingement, which our findings suggest is the most frequently occurring and therefore the most hazardous type of impingement. Patel[62] describes the same dislocating movements as observed in the current study; According to the data presented in their study, the majority of flexion movements resulted in implant-on-implant impingement, while extension movements predominantly exhibited bony impingement. In a series of 23 patients undergoing three-dimensional planning, Vigdorchik[64] demonstrated that both BOB and IOI impingements occurred during flexion movements, while IOI impingement predominated during extension movements, highlighting the significance of articulation (32mm, 36mm, Dual-mobility design).Other studies mentioned in the literature refer to simulation studies conducted using commercial software, which are used for three-dimensional planning aimed at subsequent navigated or robot-assisted total hip replacement. However, these are proprietary technologies that often do not consider bone-on-bone impingement or implant-on-bone impingement. Furthermore, although these are potentially very useful tools, they offer an approach that is not strictly scientific and reproducible. This highlights a potential gap in the existing literature and underscores the importance of including implant-on-bone impingement in future studies for a more comprehensive understanding of the issue.

Data presentation

The findings of the study have been presented in a manner designed to facilitate comprehension, also the methodological framework enhances the efficiency of interpreting intricate biomechanical data relevant to orthopaedic considerations.
These objectives were achieved by simplifying the experimental model to investigate a singular angular parameter for each dislocating motion. Additionally, the employment of a

uniform implant positioning and orientation, along with a restriction to only three sagittal plane configurations of the pelvis, substantially reduced the volume of data extracted from the experimental model, thereby enabling the selection of only the most pertinent data points. This streamlined approach serves to make the complex biomechanical data more manageable and clinically applicable.
Each table presents kinematic data corresponding to the specific motions under investigation across varying pelvic orientations, namely: Neutral Pelvis, Anteverted Pelvis, and Retroverted Pelvis. Within each of the three designated columns, angular thresholds signifying the onset of impingement are demarcated. A colour coding system is implemented to facilitate the visual differentiation between impingement-free motions (indicated in green) and motions evidencing impingement (indicated in orange). Furthermore, the angular value at which the earliest onset of impingement occurs, among the triad of examined impingement categories (implant-on-implant, implant-on-bone, and bone-on-bone), is accentuated in red.
Other simulation studies in the field of orthopedics frequently exhibit elevated levels of complexity, both in terms of their methodological approaches and the high volume of extracted data, which often lack clinical significance or are not readily comprehensible[61,62,65]. The presentation of data within this domain, specifically concerning the representation of ranges of motion, is frequently challenging, identifying a significant representative issue. Furthermore, there appears to be a lack of standardization or translational utility in how these data are conveyed. This issue complicates the interpretation and potential clinical application of such intricate biomechanical information.

CONCLUSIONS

The introduction of spinopelvic relationships in the setting of THR is a highly discussed topic in recent literature, the importance of which is now well recognized, especially in patients with pathological alterations of pelvic alignment or with limitations/rigidity of spinopelvic movements. Specific diagnostic and therapeutic pathways have indeed altered the clinical practice of hip prosthesis surgeons, allowing for the reduction of adverse events such as dislocations, instability, and impingement.

The interplay between spinal and hip anatomy has garnered substantial scholarly interest, enabling a comprehensive exploration of key aspects and clinical challenges in recent years. Although significant advances have been made in resolving many of these issues, complexities remain, particularly regarding possible therapeutic approach. Moreover, the field is marked by a notable absence of standardized objectives, terminology, and data presentation, which complicates systematic problem-solving. Existing clinical guidelines frequently fall short in providing actionable guidance, often lacking a straightforward and unambiguous approach to addressing these concerns.

The current research offers a methodologically rigorous and replicable experimental framework marked by both robustness and high fidelity to anatomical and biomechanical realities. Initial findings not only substantiate the credibility of the simulation settings but also commend the clarity and efficacy with which the data have been extracted and presented.

Upon examining the outcomes correlated with three distinct orientations of the pelvic structure, the study underscores the pivotal role that sagittal alignment of the pelvis plays in preserving the stability of prosthetic joints.

Upon examining the outcomes correlated with three distinct orientations of the pelvic structure, the study underscores the pivotal role that sagittal alignment of the pelvis plays in preserving the stability of prosthetic joints. In the present study it was discerned that a pelvic orientation in anteversion registered impingement in a greater number of movements and presented an overall reduced range of motion, thus marking itself as the most susceptible to instability and dislocation events. On the contrary, a neutral pelvic alignment demonstrated a reduced number of impingement and higher range of motion, denoting it as the least prone to impingement, instability and dislocating events.

Implant-on-bone impingements were predominantly observed. In contrast, implant-on-implant impingements were found to manifest at more extreme angles, being clinically relevant only in pure extension movement.

The results of the research are structured to aid understanding, while the methodological approach streamlines the interpretation of complex biomechanical data pertinent to orthopedic concerns.

FUTURE PERSPECTIVES

Future developments in this line of research necessitate the incorporation of simulation scenarios that encompass varying orientations of prosthetic components, or the design of "in silico trials" utilizing the inherent capabilities of the geometric model extracted from the Map client to generate a series of virtual patients with differing yet plausible morphological characteristics. The integration of soft tissues into the simulation environment, coupled with finite element analysis, will also potentially enable a more effective evaluation of the evolution of contact phenomena in terms of subluxation, dislocation, or potential damage to contact interfaces. Moreover, the incorporation of concurrent movements in both the lumbo-pelvic complex and the contralateral limb could provide a more accurate delineation of movements that are potentially at risk for instability.

REFERENCES

1. **Learmonth ID, Young C, Rorabeck C**. The operation of the century: total hip replacement. *The Lancet* 2007;370(9597):1508–1519.

2. **Sloan M, Premkumar A, Sheth NP**. Projected Volume of Primary Total Joint Arthroplasty in the U.S., 2014 to 2030. *J Bone Joint Surg Am* 2018;100(17):1455–1460.

3. **Bedard NA, Martin CT, Slaven SE, Pugely AJ, Mendoza-Lattes SA, Callaghan JJ**. Abnormally High Dislocation Rates of Total Hip Arthroplasty After Spinal Deformity Surgery. *J Arthroplasty* 2016;31(12):2884–2885.

4. **Rivière C, Lazennec J-Y, Van Der Straeten C, Auvinet E, Cobb J, Muirhead-Allwood S**. The influence of spine-hip relations on total hip replacement: A systematic review. *Orthopaedics & Traumatology: Surgery & Research* 2017;103(4):559–568.

5. **Abdel MP, Von Roth P, Jennings MT, Hanssen AD, Pagnano MW**. What Safe Zone? The Vast Majority of Dislocated THAs Are Within the Lewinnek Safe Zone for Acetabular Component Position. *Clinical Orthopaedics & Related Research* 2016;474(2):386–391.

6. **Esposito CI, Gladnick BP, Lee Y, Lyman S, Wright TM, Mayman DJ, et al.** Cup Position Alone Does Not Predict Risk of Dislocation After Hip Arthroplasty. *The Journal of Arthroplasty* 2015;30(1):109–113.

7. **Stefl M, Lundergan W, Heckmann N, McKnight B, Ike H, Murgai R, et al.** Spinopelvic mobility and acetabular component position for total hip arthroplasty. *The Bone & Joint Journal* 2017;99-B(1_Supple_A):37–45.

8. **Faldini C, Di Martino A, Borghi R, Perna F, Toscano A, Traina F**. Long vs. short fusions for adult lumbar degenerative scoliosis: does balance matters? *Eur Spine J* 2015;24(S7):887–892.

9. **Faldini C, Di Martino A, Perna F, Martikos K, Greggi T, Giannini S**. Changes in spino-pelvic alignment after surgical treatment of high-grade isthmic spondylolisthesis by a posterior approach: a report of 41 cases. *Eur Spine J* 2014;23(S6):714–719.

10. **Di Martino A, Bordini B, Ancarani C, Viceconti M, Faldini C**. Does total hip arthroplasty have a higher risk of failure in patients who undergo lumbar spinal fusion?: a retrospective, comparative cohort study from the RIPO registry. *The Bone & Joint Journal* 2021;103-B(3):486–491.

11. **Le Huec JC, Hasegawa K**. Normative values for the spine shape parameters using 3D standing analysis from a database of 268 asymptomatic Caucasian and Japanese subjects. *Eur Spine J* 2016;25(11):3630–3637.

12. **Schwab FJ, Blondel B, Bess S, Hostin R, Shaffrey CI, Smith JS, et al.** Radiographical Spinopelvic Parameters and Disability in the Setting of Adult Spinal Deformity: A Prospective Multicenter Analysis. *Spine* 2013;38(13):E803–E812.

13. **Maratt JD, Esposito CI, McLawhorn AS, Jerabek SA, Padgett DE, Mayman DJ**. Pelvic Tilt in Patients Undergoing Total Hip Arthroplasty: When Does it Matter? *The Journal of Arthroplasty* 2015;30(3):387–391.

14. **Eftekhary N, Shimmin A, Lazennec JY, Buckland A, Schwarzkopf R, Dorr LD, et al.** A systematic approach to the hip-spine relationship and its applications to total hip arthroplasty. *The Bone & Joint Journal* 2019;101-B(7):808–816.

15. **Le Huec JC, Thompson W, Mohsinaly Y, Barrey C, Faundez A**. Sagittal balance of the spine. *Eur Spine J* 2019;28(9):1889–1905.

16. **Barbier O, Skalli W, Mainard L, Mainard D**. The reliability of the anterior pelvic plane for computer navigated acetabular component placement during total hip arthroplasty: Prospective study with the EOS imaging system. *Orthopaedics & Traumatology: Surgery & Research* 2014;100(6):S287–S291.

17. **Kalifa G, Charpak Y, Maccia C, Fery-Lemonnier E, Bloch J, Boussard J-M, et al.** Evaluation of a new low-dose digital X-ray device: first dosimetric and clinical results in children. *Pediatric Radiology* 1998;28(7):557–561.

18. **Gorin M, Roger B, Lazennec J-Y, Charlot N, Arafati N, Bissery A, et al.** Hip-spine relationship: a radio-anatomical study for optimization in acetabular cup positioning. *Surgical and Radiologic Anatomy* 2004;26(2):136–144.

19. **Vigdorchik JM, Sharma AK, Jerabek SA, Mayman DJ, Sculco PK**. Templating for Total Hip Arthroplasty in the Modern Age. *J Am Acad Orthop Surg* 2021;29(5):e208–e216.

20. **Di Martino A, Rossomando V, Brunello M, D'Agostino C, Pederiva D, Frugiuele J, et al.** How to perform correct templating in total hip replacement. *Musculoskelet Surg* 2023;107(1):19–28.

21. **Lembeck B, Mueller O, Reize P, Wuelker N**. Pelvic tilt makes acetabular cup navigation inaccurate. *Acta Orthopaedica* 2005;76(4):517–523.

22. **Wan Z, Malik A, Jaramaz B, Chao L, Dorr LD**. Imaging and Navigation Measurement of Acetabular Component Position in THA. *Clinical Orthopaedics & Related Research* 2009;467(1):32–42.

23. **Innmann MM, Merle C, Gotterbarm T, Ewerbeck V, Beaulé PE, Grammatopoulos G**. Can spinopelvic mobility be predicted in patients awaiting total hip arthroplasty?: a prospective, diagnostic study of patients with end-stage hip osteoarthritis. *The Bone & Joint Journal* 2019;101-B(8):902–909.

24. **Esposito CI, Miller TT, Kim HJ, Barlow BT, Wright TM, Padgett DE, et al.** Does Degenerative Lumbar Spine Disease Influence Femoroacetabular Flexion in Patients Undergoing Total Hip Arthroplasty? *Clinical Orthopaedics & Related Research* 2016;474(8):1788–1797.

25. **Phan D, Bederman SS, Schwarzkopf R**. The influence of sagittal spinal deformity on anteversion of the acetabular component in total hip arthroplasty. *The Bone & Joint Journal* 2015;97-B(8):1017–1023.

26. **Luthringer TA, Vigdorchik JM**. A Preoperative Workup of a "Hip-Spine" Total Hip Arthroplasty Patient: A Simplified Approach to a Complex Problem. *The Journal of Arthroplasty* 2019;34(7):S57–S70.

27. **Widmer K-H**. The Impingement-free, Prosthesis-specific, and Anatomy-adjusted Combined Target Zone for Component Positioning in THA Depends on Design and Implantation Parameters of both Components. *Clin Orthop Relat Res* 2020;478(8):1904–1918.

28. **Bhaskar D, Rajpura A, Board T**. Current Concepts in Acetabular Positioning in Total Hip Arthroplasty. *IJOO* 2017;51(4):386–396.

29. **Sharma AK, Vigdorchik JM**. The Hip-Spine Relationship in Total Hip Arthroplasty: How to Execute the Plan. *The Journal of Arthroplasty* 2021;36(7):S111–S120.

30. **Kim SB, Heo YM, Hwang CM, Kim TG, Hong JY, Won YG, et al.** Reliability of the EOS Imaging System for Assessment of the Spinal and Pelvic Alignment in the Sagittal Plane. *Clin Orthop Surg* 2018;10(4):500–507.

31. **Buckland AJ, Puvanesarajah V, Vigdorchik J, Schwarzkopf R, Jain A, Klineberg EO, et al.** Dislocation of a primary total hip arthroplasty is more common in patients with a lumbar spinal fusion. *Bone Joint J* 2017;99-B(5):585–591.

32. **Di Martino A, Papalia R, Albo E, Cortesi L, Denaro L, Denaro V**. Cervical spine alignment in disc arthroplasty: should we change our perspective? *Eur Spine J* 2015;24(S7):810–825.

33. **Onggo JR, Nambiar M, Onggo JD, Phan K, Ambikaipalan A, Babazadeh S, et al.** Clinical outcomes and complication profile of total hip arthroplasty after lumbar spine fusion: a meta-analysis and systematic review. *Eur Spine J* 2020;29(2):282–294.

34. **Eneqvist T, Nemes S, Brisby H, Fritzell P, Garellick G, Rolfson O**. Lumbar surgery prior to total hip arthroplasty is associated with worse patient-reported outcomes. *Bone Joint J* 2017;99-B(6):759–765.

35. **Di Martino A, Bordini B, Geraci G, Ancarani C, D'Agostino C, Brunello M, et al.** Impact of previous lumbar spine surgery on total hip arthroplasty and vice versa: How long should we be concerned about mechanical failure? *Eur Spine J* 2023;32(9):2949–2958.

36. **Onggo JR, Nambiar M, Onggo JD, Phan K, Ambikaipalan A, Babazadeh S, et al.** Comparable dislocation and revision rates for patients undergoing total hip arthroplasty with subsequent or prior lumbar spinal fusion: a meta-analysis and systematic review. *Eur Spine J* 2021;30(1):63–70.

37. **Malkani AL, Himschoot KJ, Ong KL, Lau EC, Baykal D, Dimar JR, et al.** Does Timing of Primary Total Hip Arthroplasty Prior to or After Lumbar Spine Fusion Have an Effect on Dislocation and Revision Rates? *J Arthroplasty* 2019;34(5):907–911.

38. **Bala A, Chona DV, Amanatullah DF, Hu SS, Wood KB, Alamin TF, et al.** Timing of Lumbar Spinal Fusion Affects Total Hip Arthroplasty Outcomes. *J Am Acad Orthop Surg Glob Res Rev* 2019;3(11):e00133.

39. **An VVG, Phan K, Sivakumar BS, Mobbs RJ, Bruce WJ**. Prior Lumbar Spinal Fusion is Associated With an Increased Risk of Dislocation and Revision in Total Hip Arthroplasty: A Meta-Analysis. *J Arthroplasty* 2018;33(1):297–300.

40. **Zagra L, Benazzo F, Dallari D, Falez F, Solarino G, D'Apolito R, et al.** Current concepts in hip-spine relationships: making them practical for total hip arthroplasty. *EFORT Open Rev* 2022;7(1):59–69.

41. **Grammatopoulos G, Innmann M, Phan P, Bodner R, Meermans G**. Spinopelvic challenges in primary total hip arthroplasty. *EFORT Open Rev* 2023;8(5):298–312.

42. **Dorr LD, Malik A, Dastane M, Wan Z**. Combined anteversion technique for total hip arthroplasty. *Clin Orthop Relat Res* 2009;467(1):119–127.

43. **Dendorfer S, Weber T, Kennedy O**. Musculoskeletal Modeling for Hip Replacement Outcome Analyses and Other Applications: *Journal of the American Academy of Orthopaedic Surgeons* 2014;22(4):268–269.

44. **Kitamura K, Fujii M, Utsunomiya T, Iwamoto M, Ikemura S, Hamai S, et al.** Effect of sagittal pelvic tilt on joint stress distribution in hip dysplasia: A finite element analysis. *Clinical Biomechanics* 2020;74:34–41.

45. **Sakuma D, Ishidou Y, Fujimoto Y, Nakamura S, Ijuin T, Nagano S, et al.** Finite element analysis of mechanical stress of the hip joint in patients with posterior pelvic inclination. *World Acad Sci J* 2022;4(2):10.

46. **Joukar A, Chande RD, Carpenter RD, Lindsey DP, Erbulut DU, Yerby SA, et al.** Effects on hip stress following sacroiliac joint fixation: A finite element study. *JOR Spine* 2019;2(4):e1067.

47. **Kumaran Y, Nishida N, Tripathi S, Mumtaz M, Sakai T, Elgafy H, et al.** Effects of Sacral Slope Changes on the Intervertebral Disc and Hip Joint: A Finite Element Analysis. *World Neurosurgery* 2023;176:e32–e39.

48. **Roussouly P, Pinheiro-Franco JL**. Biomechanical analysis of the spino-pelvic organization and adaptation in pathology. *Eur Spine J* 2011;20 Suppl 5(Suppl 5):609–618.

49. Medacta Corporate | MEDACTA INTERNATIONAL. https://www.medacta.com/ , (date last accessed 30 October 2023).

50. CeramTec – The Ceramic Experts. https://www.ceramtec-group.com/en/ , (date last accessed 30 October 2023).

51. Musculoskeletal Atlas Project (MAP) Client Documentation - latest — MAP Client latest documentation. https://map-client.readthedocs.io/en/latest/ , (date last accessed 30 October 2023).

52. Mimics Innovation Suite 24 Product Update | Materialise. https://www.materialise.com/en/healthcare/mimics-innovation-suite/24 , (date last accessed 30 October 2023).

53. **Hoskins W, Rainbird S, Holder C, Stoney J, Graves SE, Bingham R**. A Comparison of Revision Rates and Dislocation After Primary Total Hip Arthroplasty with 28, 32, and 36-mm Femoral Heads and Different Cup Sizes: An Analysis of 188,591 Primary Total Hip Arthroplasties. *J Bone Joint Surg Am* 2022;104(16):1462–1474.

54. Materialise 3-matic | Software 3D per l'ottimizzazione di dati. https://www.materialise.com/it/industriale/software/3-matic , (date last accessed 30 October 2023).

55. **Cignoni P, Callieri M, Corsini M, Dellepiane M, Ganovelli F, Ranzuglia G**. MeshLab: an Open-Source Mesh Processing Tool. *Eurographics Italian Chapter Conference* The Eurographics Association, 2008;8 pages.

56. **Modenese L, Renault J-B**. Automatic generation of personalised skeletal models of the lower limb from three-dimensional bone geometries. *J Biomech* 2021;116:110186.

57. **Delp SL, Anderson FC, Arnold AS, Loan P, Habib A, John CT, et al.** OpenSim: open-source software to create and analyze dynamic simulations of movement. *IEEE Trans Biomed Eng* 2007;54(11):1940–1950.

58. **Seth A, Hicks JL, Uchida TK, Habib A, Dembia CL, Dunne JJ, et al.** OpenSim: Simulating musculoskeletal dynamics and neuromuscular control to study human and animal movement. Schneidman D, ed. *PLoS Comput Biol* 2018;14(7):e1006223.

59. OpenSim - Home. https://opensim.stanford.edu/ , (date last accessed 30 October 2023).

60. **Nadzadi ME, Pedersen DR, Yack HJ, Callaghan JJ, Brown TD**. Kinematics, kinetics, and finite element analysis of commonplace maneuvers at risk for total hip dislocation. *J Biomech* 2003;36(4):577–591.

61. **Pryce GM, Sabu B, Al-Hajjar M, Wilcox RK, Thompson J, Isaac GH, et al.** Impingement in total hip arthroplasty: A geometric model. *Proc Inst Mech Eng H* IMECHE, 2022;236(4):504–514.

62. **Patel AB, Wagle RR, Usrey MM, Thompson MT, Incavo SJ, Noble PC**. Guidelines for implant placement to minimize impingement during activities of daily living after total hip arthroplasty. *J Arthroplasty* 2010;25(8):1275-1281.e1.

63. **Innmann MM, Weishorn J, Beaule PE, Grammatopoulos G, Merle C**. Pathologic spinopelvic balance in patients with hip osteoarthritis : Preoperative screening and therapeutic implications. *Orthopade* 2020;49(10):860–869.

64. **Vigdorchik JM, Sharma AK, Madurawe CS, Elbuluk AM, Baré JV, Pierrepont JW**. Does Prosthetic or Bony Impingement Occur More Often in Total Hip Arthroplasty: A Dynamic Preoperative Analysis. *J Arthroplasty* 2020;35(9):2501–2506.

65. **Tang H, Li Y, Zhou Y, Wang S, Zhao Y, Ma Z**. A Modeling Study of a Patient-specific Safe Zone for THA: Calculation, Validation, and Key Factors Based on Standing and Sitting Sagittal Pelvic Tilt. *Clin Orthop Relat Res* 2022;480(1):191–205.